Chapter 2
Tail Regeneration: Ultrastructural and Cytological Aspects

Despite the numerous histological studies on regenerating tails, few ultrastructural studies have been conducted on the progressive stages of the process. These studies would allow a better identification of the modification of injured tissues and of the different cell types activated during the process of wounding. No ultrastructural studies are available for the wounding and the limited tissue regeneration of the limb.

Only the regenerating spinal cord has received a detailed transmission electron microscopy (TEM) analysis (Simpson 1968; Egar et al. 1970; Turner and Singer 1973; Alibardi 1990–1991). Other ultrastructural studies have been conducted on the differentiation of the main tissues in the tail (see later). These studies have permitted us to determine precisely the types of cells involved in the formation of the regenerative blastema in lizards and the proliferative potential of cells of the connective, ependymal, muscular, and blood tissues.

The following sections provide a summary of published and unpublished observations on the fine structure of the wounded and regenerating tissues of different species of lizards. More details can be found in specific publications cited in the following sections.

2.1
Wound Healing to Blastema Formation

Despite the extensive injuries following tail or limb amputation in lizards, the animals rarely acquire infections, a phenomenon almost impossible in a mammal. How can lizards cope with microbe penetration across their extensively exposed tissues? Ultrastructural analysis has shown that the injured stump is covered with bacteria of different types (Alibardi 2009a; Fig. 2.1a, b). Despite the contact with a dirty substratum in the terrarium, lizards rarely develop infections. These observations have shown that numerous neutrophils are present among the wound epithelium and are also located beneath the scab, where they actively engulf bacteria.

At about 2 days after amputation, many degenerating endings of sectioned muscles are seen, and numerous white blood cells are infiltrated among the

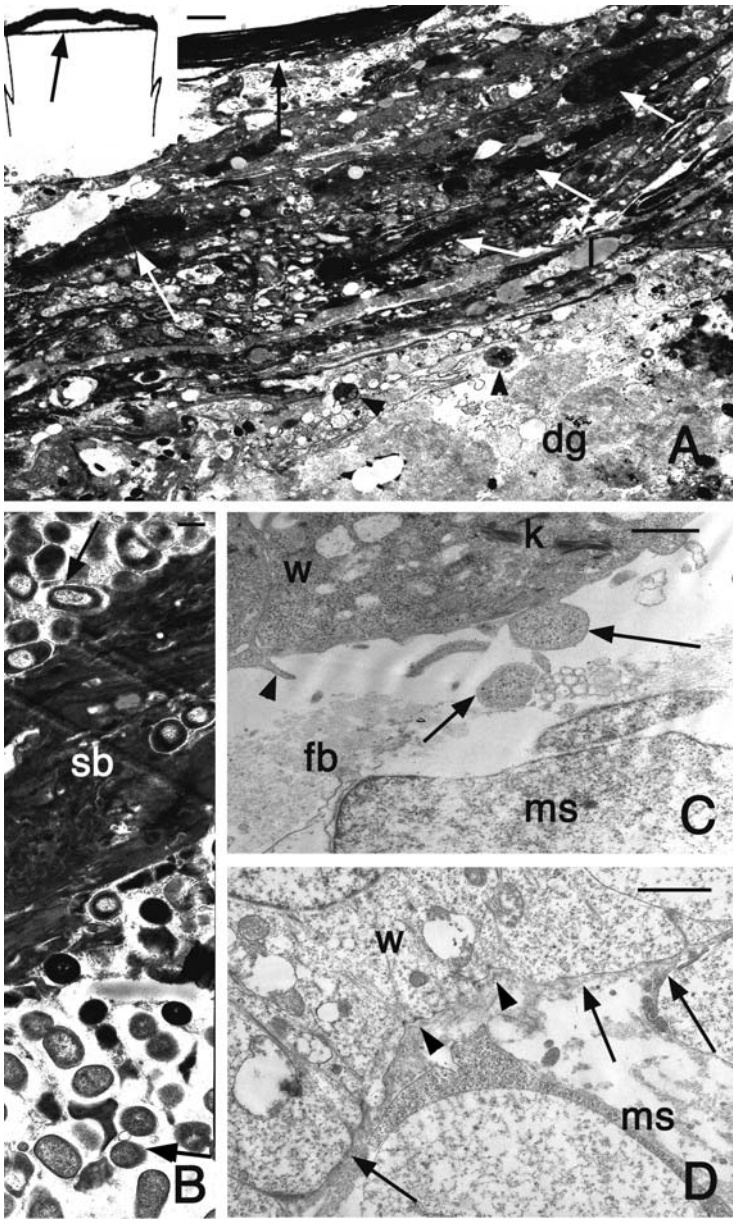

Fig. 2.1 Ultrastructural details of the tail stump (location indicated by the *arrow* in the *inset* in **a**) in *Podarcis sicula* (**a**–**c**) and *Anolis carolinensis* (**d**). **a** Aspect of the scab at 4 days after wounding. Beneath the compact outer stratum (*dark arrow*) numerous degenerating cells (*white arrows* indicated electron-dense nuclei), keratinocytes, and blood-derived cells with numerous vacuoles are accumulating. Degenerating pale cells underneath represent

connective and adipose tissues, for an extension up to 0.2–0.3 mm within the stump. The surface of the stump of the tail is initially covered with a blood clot, derived from the accumulation of blood cells over the sectioned tissues (Figs. 1.4a, 2.1a). At 3–4 days after amputation, the keratinocytes from the last sectioned scales have migrated over part of the stump but do not completely cover the stump surface (Alibardi and Sala 1983; Alibardi and Toni 2005; Alibardi 2009a).

The scab is made of electron-dense, largely amorphous material derived from platelets, and erythrocytes accumulate over injured tissues during the first few hours after lesion. Numerous bacteria (*Bacillus* sp., *Staphylococcus* sp., sometimes also *Mycobacterium* sp. with a capsule) are seen externally, but also within the scab (Fig. 2.1b). Bacteria in the phase of cell division are often seen. The scab contains numerous pycnotic nuclei, 0.1–2.0-μm lipid-like vesicles and degenerating leukocytes with digestive lysosomes, especially in contact with the wounded tissues underneath. The microbes are engulfed in digestive vacuoles of leukocytes localized among the migrating keratinocytes. The leukocytes contain 0.1–0.5-μm dense granules with a "spongy-like" texture that resemble the azurophilic granules of neutrophil granulocytes in mammals. Other dense granules instead resemble the specific granules of eosinophils/heterophils, as they contain denser particulate/polygonal structures among a less dense material.

The phagocytic keratinocytes contain few keratin bundles, desmosomal junctions, and scattered phagosomes or pale digestive vacuoles of 0.2–0.5 μm together with short vesicles of the rough endoplasmic reticulum. Although the plasma membrane of granulocytes and migrating keratinocytes is often apposed one to another, no desmosomal junctions are present between these cell types. At 12–14 days after amputation the wound epidermis comprises six to ten layers of spinous-like keratinocytes with euchromatic nuclei, located beneath a corneous layer made of five to eight layers of thin corneocytes. The flattening keratinocytes of the more external layers contain numerous short keratin bundles that tend to merge together in precorneous keratinocytes (Alibardi 1995c, Alibardi and Toni 2005). Beneath the corneous layers of forming scales, a granulated (clear) layer is formed, which forms a characteristic serrated interface with the next layer produced underneath, called the oberhautchen layer. The granulated and the new oberhautchen layers will form the splitting line for the shedding of the wound

Fig. 2.1 (continued) granulocytes containing dense granules (*arrowheads*). *Bar* 1 μm. **b** Detail of scab at 5–6 days with condensed cell material surrounded by bacteria (*arrows*). *Bar* 200 nm. **c** Detail of the basal part of the wound epithelium contacting the underlying connective tissue at 7–8 days after wounding. Two cytoplasmic blebs (*arrows*) and a microvillar elongation (*arrowhead*) from migrating keratinocytes are seen. *Bar* 1 μm. **d** Detail showing the dermal–epidermal boundary of the blastema at 16 days after amputation. The dense lamella is largely incomplete (*arrowheads*), whereas an amorphous material (*arrows*) occupies most of the incomplete basement membrane. *Bar* 1 μm. *dg* degenerating granulocytes, *fb* fibrin exudate, *k* keratin bundles, *l* lipid vesicle, *msn* mesenchymal cell, *sb* scab material, *w* wound keratinocytes

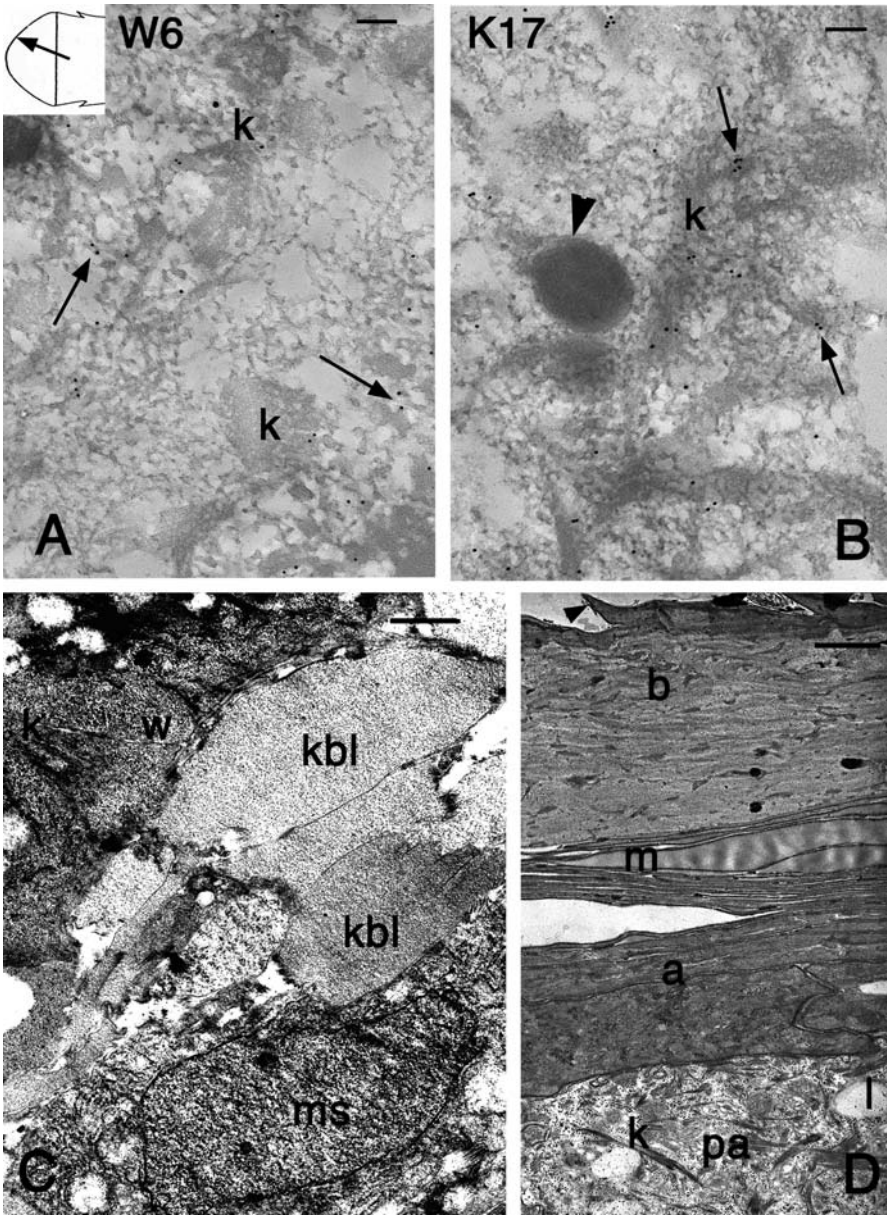

Fig. 2.2 Ultrastructural detail of cells of the wound epidermis (**a**–**c**) in the blastema (*arrow* in the *inset* in **a**) and regenerated epidermis of the new scales (**d**) in *P. sicula*. **a** Diffuse immunogold labeling (*arrows*) for wound antigen 6 among keratin bundles. *Bar* 100 nm. **b** Diffuse immunogold labeling for keratin 17 (*arrows*) among keratin bundles. The *arrowhead* points to a dense granule. *Bar* 100 nm. **c** Cytoplasmic blebs of the basal cells

epidermis (Alibardi 1998, 1999, 2001). The process of shedding is favored by the degradation of cell junctions between granulated and oberhautchen layers as indicated by the activity and localization of acid phosphatase contained in the lysosomes of these cells.

In the tail blastema, the basement membrane of the wound epidermis, in particular the dense lamella appears discontinuous and some cytoplasmic blebs of migrating keratinocytes are seen (Fig. 2.1c, d). Elongating keratinocytes show numerous microvillar extensions contacting the loose exudates and the few collagen fibrils with no banding present in the healing connective tissue.

Wound keratinocytes contain short endoplasmic cisternae, irregular pale vesicles, lipid droplets, and sparse, round, and dense granules of 0.1–0.4 μm. The short keratin bundles of wound keratinocytes are diffusely immunolabeled for wound keratins 6, 16, and especially 17, like in mammalian wound keratinocytes (McGowan and Coulombe 1998; Alibardi and Toni 2005, 2006; Fig. 2.2a). Keratin 17 is a special keratin believed to favor the movement of migrating keratinocytes as it is linked to elastic elements of their cytoskeleton (actin, etc.) Migrating and stratifying keratinocytes of the wound epidermis are also react toward wound antigen 6, a typical cytoskeleton-associated marker associated with the regenerating wound epithelium of amphibians (Estrada et al. 1993; Fig. 2.2b). Immunogold labeling at the TEM level has shown that the antigen is diffuse in the cytoplasm and associated with keratin bundles. The immunogold labeling shows that the keratin 17 antibody tends to label loosely the periphery of the short keratin bundles of lizard wound keratinocytes but not the entire bundle (Alibardi and Toni 2005). The long bundles most likely contain other keratin types. Both these cytoskeletal proteins, wound antigen 6 and keratin 17, are associated with the short keratin bundles of migrating keratinocytes, and are absent in stabilized keratinocytes of normal epidermis (Geraudie and Ferretti 1998).

The basal layer of the wound epidermis often appears irregular, and this is due to the numerous cytoplasmic blebs produced by basal keratinocytes in the initial wound epithelium of the blastema at 8–12 days after amputation (Alibardi 1994b, 1999). Often this part of the epithelium is so irregular and the boundary between epithelial and mesenchymal cells is quite indistinct that some cells may actually detach from the epithelium to move into the mesenchyme through a process known as epithelial–mesenchymal transformation (Hay 1996; Fig. 2.2c).

Fig. 2.2 (continued) of the wound epidermis in contact with mesenchymal cells of the blastema. *Bar* 1 μm. **d** Restored epidermal layer sequence after loss of the wound epithelium in regenerated scale. The *arrowhead* indicates a spinule of the external oberhautchen layer which is merged with the electron-pale β-layer, separated by thin mesoS cells from the differentiating α-layer underneath. *Bar* 0.5 μm. *a* α-layer, *b* β-keratin layer, *k* keratin bundle, *kbl* basal bleb of keratinocytes, *K17* keratin 17 immunolabeling, *l* lipid droplet, *m* mesoS (intermediate) layer, *ms* mesenchymal cell of the blastema, *pa* pre-α (differentiating) cell, *W6* wound antigen 6 immunolabeling, *w* cells of the wound epithelium

Within the wound epidermis a shedding layer is gradually formed. The upper part of the wound epidermis is lost and new cells derived from the basal layer will form the hard, β-keratin layers of the new epidermis (Figs. 1.1o, 2.2d).

The inflammatory process in lizards has some differences from the cellular response present in mammals. In the latter, granulocytes degenerate in 1–3 days and are replaced by macrophages of blood origin in the following days which become the more common phagocytes in wounds (Kovacs and DiPietro 1994; VanDen Boom et al. 2002; Wynn 2008). Differently, in wounded reptilian tissues most leukocytes and only a few macrophages colonize the injured area during the first week, and leukocytes persist in high number in the inflamed area for a long time (Montali 1988; Huchezermayer and Cooper 2000; Tuchunduva et al. 2001; Alibardi 2009a). These cells are recruited from the blood, as is also indicated from some lowering of their number in the blood during the preblastematic and early stages of tail regeneration (Hiradar et al. 1979; Shah et al. 1980). The longer permanence of granulocytes that have migrated into the wound tissues in reptiles in comparison with mammalian wounds (Montali 1988; Smith and Barker 1988; Tuchunduva et al. 2001; Alberio et al. 2005) may also indicate that these cells survive longer than in mammals. Macrophages are less frequent during the first 4–6 days after amputation, and beneath the scab of the stump the second main line of defense is represented by granulocyte heterophils. The numerous azurophil granules, and the specific granules, may contain potent antimicrobial molecules that remain to be specifically identified. However, the cellular and molecular nature of this innate immunity, whether present in regenerating keratinocytes or/and in the underlying white blood cells in lizard wounds, is not known. Can lizards produce antimicrobial molecules responsible for the relatively low and brief inflammatory reaction that favor tissue regeneration? Innate molecules such as defensins and cathelicidins are not known in lizards, but they have been described in amphibians and the chick (Zasloff 2002). The presence of putative, antimicrobial molecules in injured lizard tissues and their potential pharmacological role remain to be discovered.

Beneath the wound epidermis, migrating chromatophores such as lipophores, iridophores, and melanophores are often present. Typical mesenchymal (blastema) cells accumulate beneath the wound epithelium at 12–14 days after amputation, and very little amorphous material (glycosaminoglycans) and scarce, nonbanded thin collagen fibrils are present (Alibardi and Sala 1988a, b, 1989). Around the ependymal ampulla, cells of mesenchymal aspect actively take up tritiated thymidine (Fig. 2.3a) and proline (Fig. 2.3b). Although they are surrounded by numerous collagen fibrils, proliferating fibroblasts are also present in the lesioned meninges and in the regenerating dermis (Fig. 2.3c).

The ultrastructural aspect of blastema cells is essentially summarized in the variation of shape and extent of surface elongation, from fusiform cells (fibroblast-like) toward a more irregular mesenchymal aspect, and in the variable amount of rough endoplasmic reticulum that is present in these cells (Alibardi 1986, 2009b; Alibardi and Sala 1988a, b, 1989). These cytological aspects and the

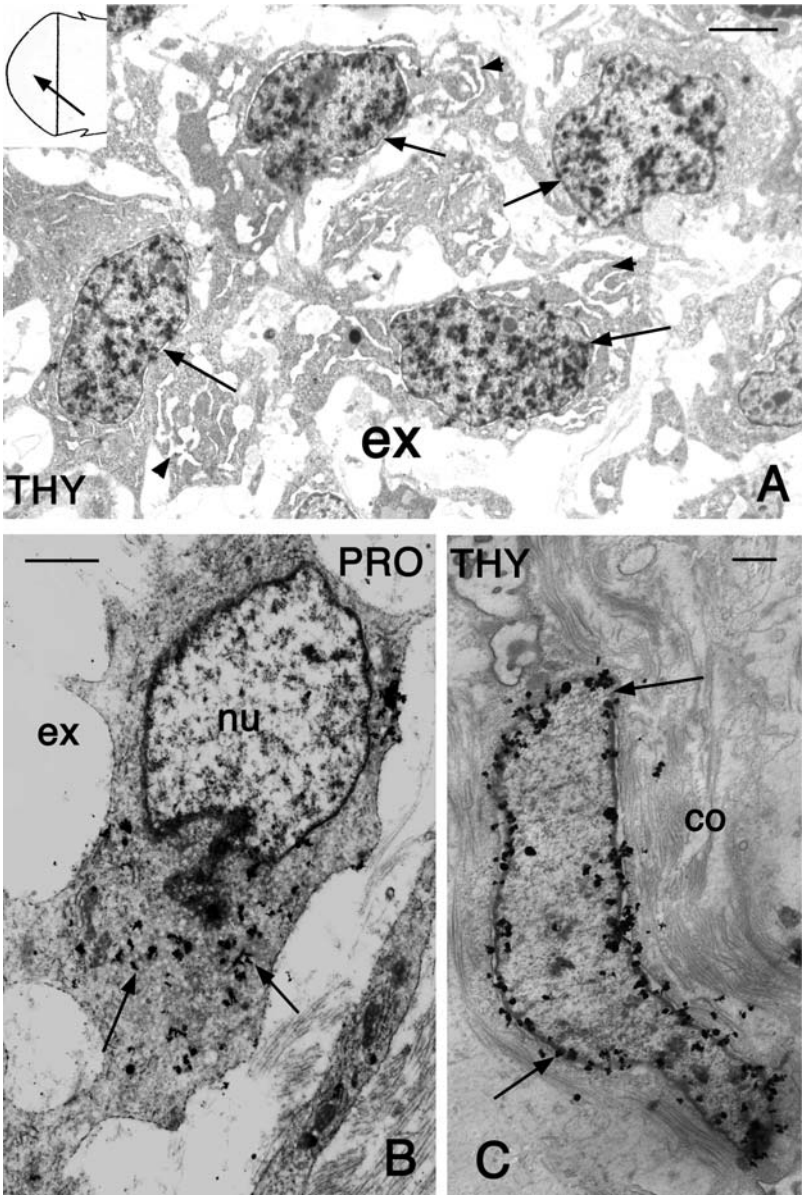

Fig. 2.3 Ultrastructural aspects of cells of the regenerative blastema in *A. carolinensis* (**a**, **c**) and *Lampropholis delicata* (**b**). **a** Mesenchymal cells with tritiated thymidine labeled nuclei (*arrows*) present in the central region of the blastema (*arrow* in the *inset*). *Arrowheads* indicate regions of the cytoplasm with developed ergastoplasmic cisternae. *Bar* 2.5 μm. **b** Labeled cell (*arrows*) 1 h after injection of tritiated proline, located at the apex of the regenerating meninx. *Bar* 2 μm. **c** Thymidine-labeled fibroblast in the more lateral region (dermal) of the blastema. *Bar* 1 μm. *co* collagen fibrils, *ex* extracellular space, *nu* nucleus, *PRO* tritiated proline autoradiography, *THY* tritiated thymidine autoradiography

cell density within the tail blastema and cone are probably related to the tissue derivation. In the center of the blastema, mesenchymal cells have a poorly developed ergastoplasm, but those located around or as a continuation of the apical ependymal ampulla contain numerous endoplasmic cisternae. The latter probably represent meningeal cells or even detached ependymal cells. In the area of promuscle aggregates, mesenchymal cells frequently divide, and appear labeled after 4 h to 1 day after injection of tritiated thymidine. They appear well labeled after injection of tritiated proline, indicating that these cells possess an active metabolism. In the lateral area of the blastema, where the dermis will be formed, some typical fibroblasts surrounded by few collagen fibrils are present, often incorporating tritiated thymidine. In all the regions of the tail blastema however, the extracellular matrix is very scarce and contains mainly amorphous material, probably glycosaminoglycans, and collagen fibrils are scarce and generally do not form banded bundles.

Numerous cell types are present among mesenchymal cells of the blastema, in particular macrophages, hematogenous cells (immature red blood cells or other types of blood cells), and melanophores. In conclusion, it is clear from the above description that a limited inflammatory reaction with a relatively low number of leukocytes and macrophages occurs along the autotomy planes of the tail. This condition favors the accumulation of mesenchymal cells of different origin, and perhaps also the wound epithelium can provide cells of the blastema through an epidermal–mesenchymal transformation. The latter phenomenon and its quantitative contribution to the cell population of the regenerative blastema in lizard regeneration has still to be evaluated. Typical of the tail blastema is the close association between mesenchymal and epithelial cells due to the discontinuous basement membrane, an aspect that indicates an intense dermal–epidermal interaction during these stages.

2.2 Tissue Differentiation

2.2.1 Epidermis

The wound epidermis at 1–2 mm from the tail tip is covered by five to eight layers of mature corneocytes, whereas the living keratinocytes form a waved epidermis (Figs. 1.4k, 1.6a). After the formation of deep epidermal pegs (Fig. 1.6c–e), the epidermis undergoes cell differentiation to produce the typical stratification of normal scales (Maderson et al. 1978; Maderson 1985; Alibardi 1995a, 1998, 2001). The wound epidermis is an immature α-keratin layer and the formation of the granulated layer occurs by the accumulation of keratohyalin-like granules of 0.1–4.0 μm in diameter (depending on the species; see Alibardi 1999, 2001). Numerous dense granules of submicroscopic dimension (0.1–0.2 μm) are

produced in upper wound keratinocytes before they pack into the corneous layer (Fig. 2.2b). When it matures, the granulated layer (known as the clear layer) forms interdigitations with the next layer (the oberhautchen layer), along which the epidermis of the pegs splits into two parts producing new scales (Fig. 1.6e–g). Beneath the oberhautchen layer, all the new epidermal layers of the regenerated (or neogenic) scales are formed, like in normal scales: the hard β-layer, the water-loss-limiting mesos layer, and the flexible α-layer (Fig. 2.2d; Maderson and Roth 1972; Maderson 1985; Alibardi 1995c, 2000).

Both acidic and basic keratins are present in the regenerating epidermis and the molecular mass of these proteins varies from 40 to 63 kDa (Alibardi et al. 2000). When the oberhautchen and β-layers are produced, they accumulate a large amount of a hard type of keratin, termed β-keratin. α-Keratins (soft) remain in the mature β-layer but are the prevalent keratins of the softer α-layers produced underneath the β-keratin layer. The formation of neogenic scales (regenerated) that show the same sequence of epidermal differentiation as in normal epidermis has become an essential model to analyze the molecular biology of corneous proteins in the reptilian skin. In fact, from regenerating scales, the genes coding for epidermal keratins were determined for the first time (Dalla Valle et al. 2005). Since the initial sequences were obtained, it has been easier to clone and sequence these proteins from all reptilian groups.

Few studies on regenerated skin have illustrated the complete differentiation not only of a normal epidermis but also of some epidermal specializations (Maderson 1971). These consist of sense organs (likely mechanoreceptors) or modified scales with pads made of microscopic hairy-like bristles (likely touch-sensorial or capable of adhesion to the substrate), and even some glandular structures. In some climbing geckos, numerous regenerated scales of the central area of the tail reform extensive, pad-like areas of adhesion, which are made of millions of setae, like those present in the original tail. These modified scales help the tail to tightly grasp and adhere to the substratum represented by tree branches and other rough surfaces (Bauer 1998).

2.2.2 Blood Vessels, Fat, and Meninges

After the stage of blastema formation, various tissues differentiate and grow, so sustaining the elongation of the new tail, among which there is a new vasculature, pericartilaginous fat deposits, and, more internally, meninges around the new spinal cord.

The anatomical details of the vascular network that is established in the regenerating blastema and in the elongating tail are not specifically known, but the initial vascularization of regenerating tissues is likely irregular as in the regenerative blastema of the newt (Peadon and Singer 1966). Numerous endothelial cells take up tritiated thymidine in the blastema, giving rise to narrow

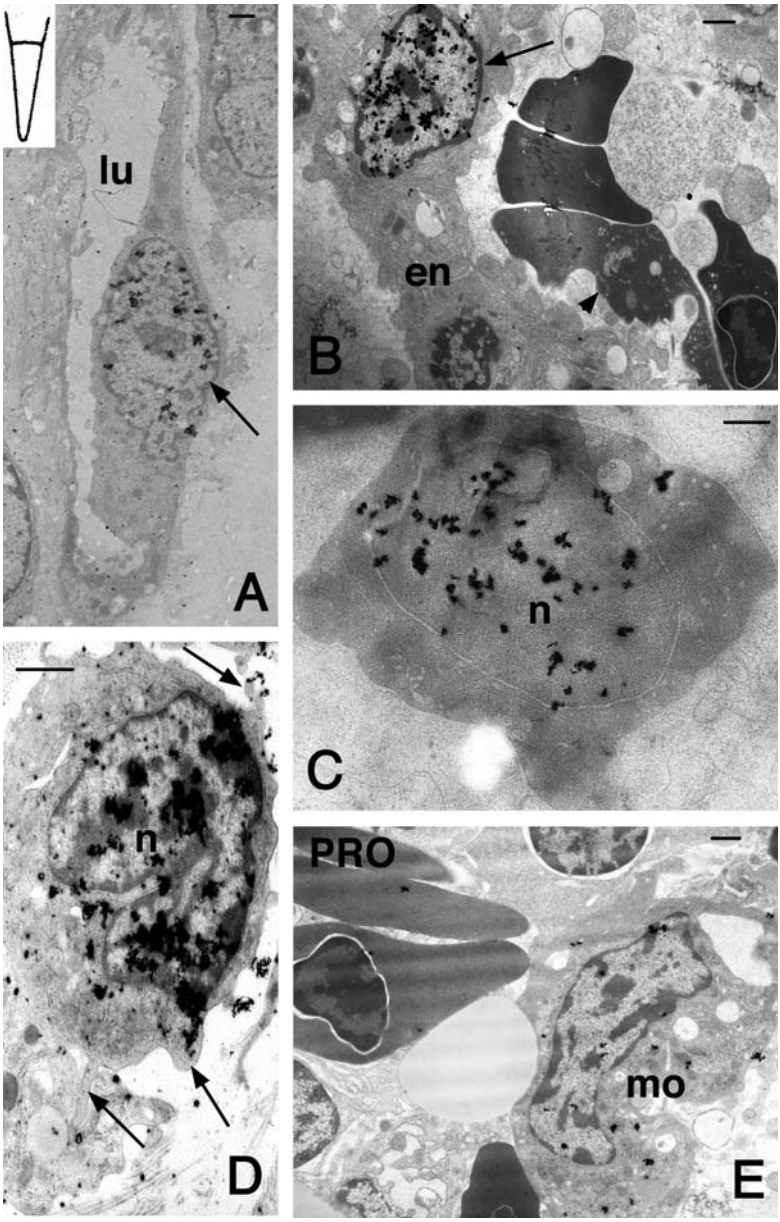

Fig. 2.4 Blood cells in regenerating tail (correspondent stage indicated in the *inset* in **a**) of *A. carolinensis* (**a–d**) and *L. delicata* (**e**). **a** Tritiated thymidine labeled nucleus of endothelial cells (*arrow*) among the blastema of the regenerating tail (the *inset* shows the approximative stage). *Bar* 0.5 μm. **b** Tritiated thymidine labeled, immature blood cells (*arrow*) in a blood island (the *arrowhead* indicates compacted erythrocytes) located at the

capillaries or to the large lacunae initially present (Hughes and New 1959; Alibardi 1993b; Fig. 2.4a, b). The initial blood vessels are of the fenestrated type and form broad lacunae among blastema cells and around the apical ependymal ampulla. Therefore, no tight blood–brain barrier is initially present in the early regenerating spinal cord, and small to medium-sized molecules such as amino acids, and likely also higher molecular weight molecules, may freely move from the blood into the nervous system and vice versa. From the apical sinusoid vessels present in the blastema, mature or immature red and white blood cells can move into the blastema, comprising polychromatophilic and orthochromatophilic erythroblasts and monocytes.

Inside these capillaries or in the larger sinusoids, red blood cells often appear not completely mature and still capable of multiplication, as is indicated by the uptake of tritiated thymidine (Fig. 2.4b, c). The increased hematopoiesis activity, elicited by the process of regeneration (Ramachandran et al. 1983; Shah et al. 1980), has allowed the erythropoietic span in lizards to be determined (Alibardi 1994c). In the lizards *Lampropholis delicata* and *Anolis carolinensis* the erythropoiesis is initiated in the bone marrow and continues during tail regeneration, also in the bloodstream. The stage from erythroblasts to orthochromatophilic nucleated erythroblasts lasts about 14 days, about twice as long as in some homeothermic amniotes (mammals) of the stage from erythroblasts to reticulocytes. It is also likely that both red and white blood cells can divide within the bloodstream during tail regeneration. Monocytes and macrophages incorporating tritiated thymidine have also been seen within the blood vessels and even in the regenerating blastema (Fig. 2.4d), but the importance of extramarrow cell multiplication of blood cells during lizard regeneration is not known. Many monocytes within blood vessels also incorporate high levels of tritiated proline, in relation to their high metabolism in comparison with a lower metabolic activity of immature or mature red blood cells (Fig. 2.4e).

Although they exist in lower numbers than blood vessels, lymph vessels are also regenerated during tail regeneration, as is illustrated for the gecko *Christimus marmoratus* (Daniels et al. 2003). During the first 3 weeks of tail regeneration, the flux of lymph is slower than in the normal tail. Lymph vessels are more actively formed from 3 to 9 weeks of regeneration, as also indicated by the activation of the vascular endothelial growth factor during this period. Most lymph vessels are localized in the subcutis, between the dermis and the underlying regenerating muscles, and carry the lymph to the liver and then to the heart.

Fig. 2.4 (continued) tip of the regenerating tail. *Bar* 0.5 μm. **c** Thymidine-labeled nucleus of proerythroblasts in the blastema. *Bar* 1 μm. **d** Thymidine-labeled nucleus of a macrophage in the blastema (*arrows* indicate cytoplasmic blebs). *Bar* 1 μm. **e** Tritiated proline labeled monocyte migrating into the blastema from a sinusoid blood vessel. *Bar* 1 μm. *cy* cytoplasm, *er* erythrocytes, *lu* lumen of the capillary, *Mo* monocyte (macrophage), *n* nucleus, *PRO* tritiated proline autoradiography

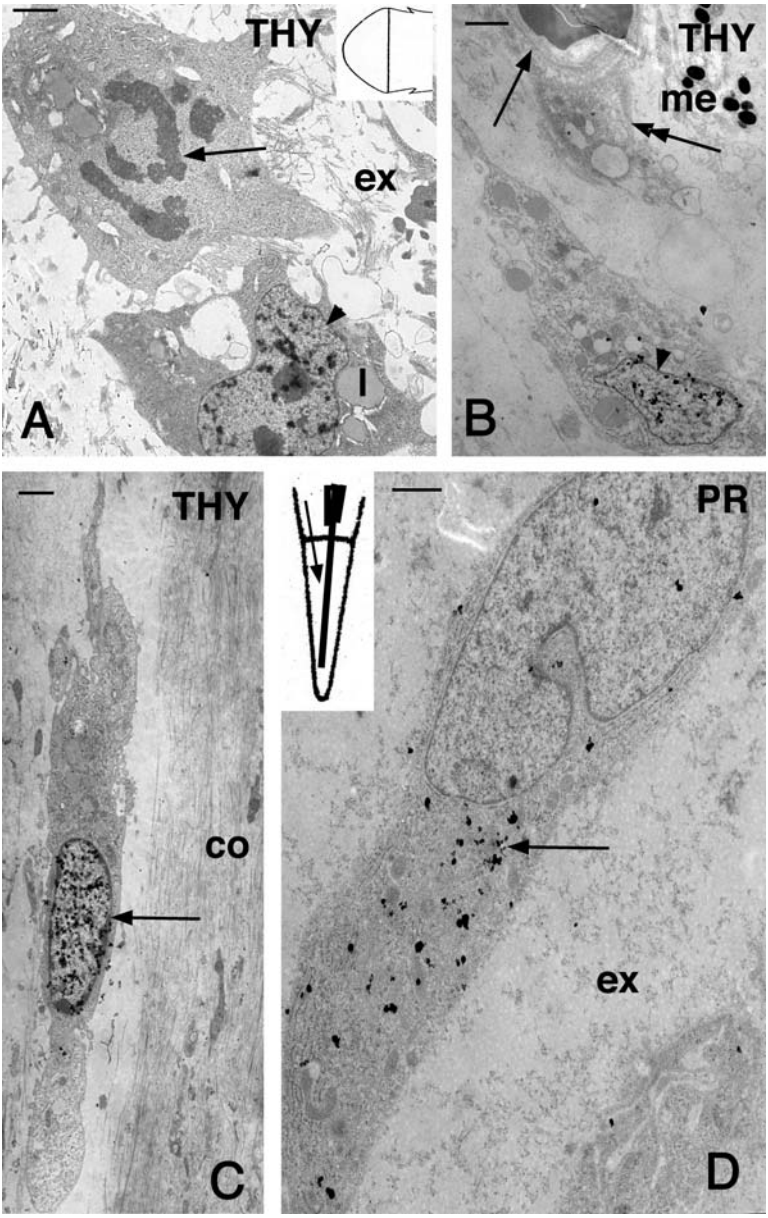

Fig. 2.5 Differentiating lipocytes in pericartilaginous regions (**a**, **b**) and meningeal cells surrounding the regenerating spinal cord (**c**, **d**). **a** Dividing cell (*arrow* on chromosomes) present within the mesenchyme close to a lipoblast with a tritiated thymidine labeled nucleus in *A. carolinensis*. *Bar* 1 μm. The *inset* shows the stage of regeneration. **b** Other thymidine-labeled lipoblasts (*arrow*) with numerous lipid droplets close to a blood vessel

In proximal regions of the elongating tail, capillaries, arterioles, and venules around the spinal cord mature into tight vessels owing to the disappearance of gaps in the endothelium and to the formation of tight junctions between endothelial cells. The latter are completely surrounded by a continuous basement membrane. These changes are observed in regenerated tails after 1 month of regeneration, and the blood vessels then now similar to those of the normal tail. The vessels are connected to the axial, caudal (dorsal) artery, from which they probably originated, and eventually join to the two main caudal veins. The process of angiogenesis appears also related to the formation of the fat tissue in the new tail.

At the stage of the elongating cone (Fig. 1.1l), in the region located between the differentiating muscles and the cartilage (Fig. 1.1m), numerous fibroblast-shaped cells often associated with blood vessels show labeled nuclei after injection of tritiated thymidine (Fig. 2.5a, b). These cells often contain small lipid droplets (0.3–1.0 μm) that indicate they are dividing lipoblasts (Alibardi 1995d). The number of fat cells and their lipid content rapidly increase, and the initial series of metameric adipomers (at least in *L. delicata*) later disappears to be replaced by an apparently unique mass of fat tissue that surrounds the cartilaginous tube. As a result, the adipose tissue is more abundant in the fully regenerated tail than in the native tail. Differentiated lipocytes retain the thymidine label, indicating that they do not frequently multiply when differentiation is under way. However, some lipocytes with large lipid droplets are still capable of taking up tritiated thymidine at 4 h after injection, suggesting that they can still divide.

Aside from the uptake of tritiated thymidine in their nuclei, lipoblasts also take up tritiated proline, which concentrates in the ergastoplasm, indicating not only an active cell division but also protein synthesis at early stages of tail elongation. The burst of cell division mainly occurs in cells of the submuscular connective tissue, 1–2 mm distant from the tip of the regenerating tail. The initial small lipid droplets rapidly merge into large droplets that occupy most of the cell at maturity until a unilocular cell is formed in proximal regions of the regenerated tails around 1 month from the beginning of tail regeneration.

Around the apical regions of the regenerating spinal cord, within 1–2 mm from the tail tip, mesenchymal cells tend to flatten and these cells become surrounded by numerous collagen fibrils (Fig. 2.5c, d). These flat fibroblasts actively take up tritiated thymidine and especially proline, indicating these cells are metabolically more active than the mesenchymal type from which they derive, and are still capable of intense cell multiplication. The numerous, tendentially oriented

Fig. 2.5 (continued) (*arrowhead*) in *L. delicata*. *Bar* 1.5 μm. **c** Flat meningeal fibroblast with a tritiated thymidine labeled nucleus (*arrow*) in *A. carolinensis*. *Bar* 1 μm. **d** Meningeal fibroblast actively synthesizing collagen as indicated by the tritiated proline labeling (*arrows*) in the cytoplasm (*L. delicata*). The *inset* gives the indicative position of this cell around the spinal cord (*arrow*). *co* collagen fibrils, *l* lipid droplet, *ex* extracellular matrix, *me* melanocyte, *n* nucleus, *PR* tritiated proline autoradiography image, *TH* tritiated thymidine autoradiography image

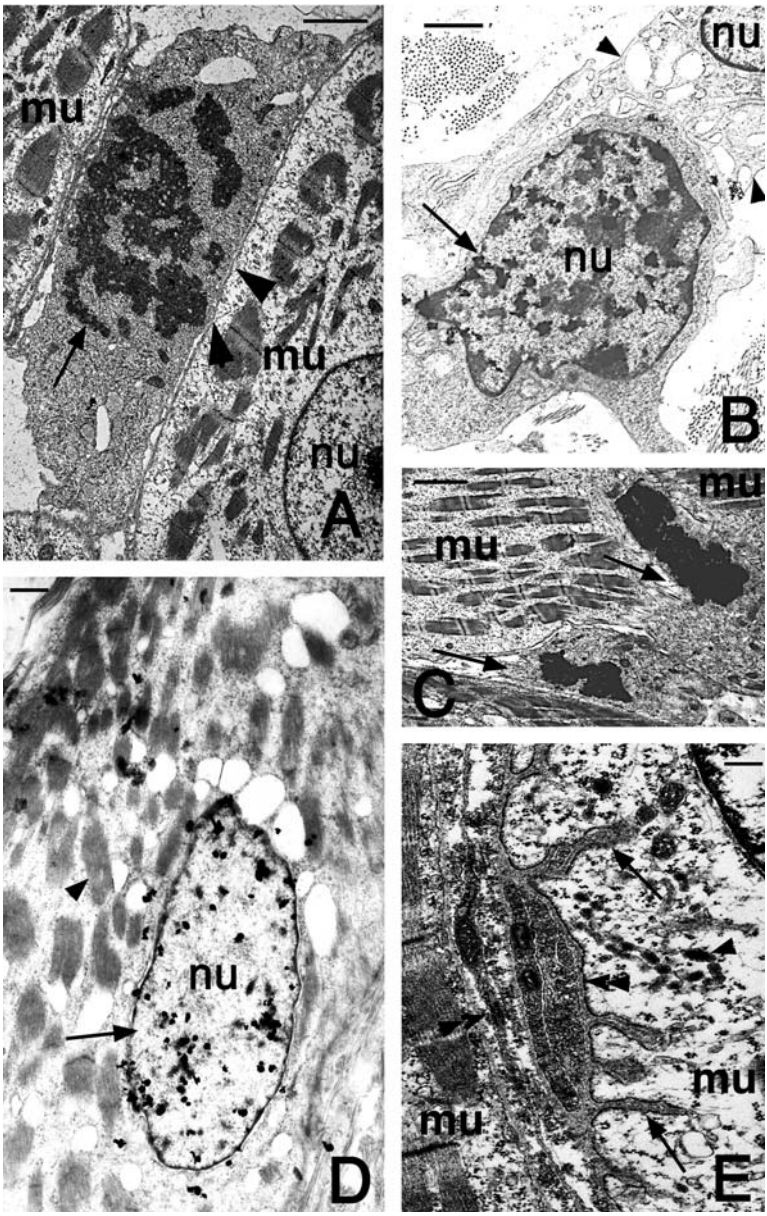

Fig. 2.6 Ultrastructural detail of regenerating muscles in elongating tails of *A. carolinensis* (**a, b**) and *L. delicata* (**c–e**). **a** Dividing cell (*arrow* on forming chomosomes) that is likely merging (*arrowhead*) with regenerating muscle cells. *Bar* 1 μm. **b** Thymidine-labeled nucleus of a myoblast in the phase of fusion (*arrowheads*) with another myoblast (4 h after injection). *Bar* 1 μm. **c** Detail of a dividing cell (*arrows* point to the nuclei in telophase)

collagen fibrils along the axial ependyma form a relatively regular dense connective tissue surrounding the spinal cord (Fig. 2.8b). These fibers are likely involved in mechanically sustaining the new spinal cord during the bending movements of the tail. This hypothesis is also suggested by the case of meningeal regeneration in the New Zealand gecko *Hemidactylus maculates*. In this species, the meningeal fibroblasts of the regenerated spinal cord synthesize a large amount of elastin and are eventually surrounded by numerous and large elastic fibrils in addition to collagen fibrils (Alibardi and Meyer-Rochow 1989). In this species, the regenerated tail is commonly curled up around objects of tree branches. This activity might result in the bending or tearing of the regenerated spinal cord within the cartilaginous tube. The presence of an elastic meninx inside the curling elastic cartilaginous tube in the regenerated tail of this species allows the functionality of the tail without damaging the delicate spinal cord.

2.2.3 Muscles

In case of autotomy, muscle regeneration in the blastema derives from stem cells localized in the autotomy septum, adjacent to satellite cells of the stump muscles (Bayne and Simpson 1977). Therefore, it is likely that myogenic cells derived from satellite cells of old muscles can detach from the fiber after lesion, migrate to the stump, and contribute to the formation of a blastema. Later, these cells reform the new muscles. Although myoblasts merge in vivo, they can still synthesize DNA, and DNA synthesis also seems to occurs in some of the nuclei already incorporated in myotubes (Alibardi 1995e). Tritiated thymidine labeled nuclei and mitotic nuclei are mainly present near the myosepta or in the more external parts of the myotome (Fig. 2.6a–c). This observation suggests that the growth of the regenerating muscle fibers mainly occurs in the area contacting the myosepta. An in vivo autoradiography study has indicated that new myocells penetrate into the myotube in 2–3 days, and that centrally located and labeled nuclei are seen after 12 days from the injection of tritiated thymidine (Fig. 2.6d).

When the regenerating tail is more than 1 cm long, in the lizard *Podarcis muralis*, in the skink *Gonglylus gongylus* (Filogamo and Marchisio 1961), as well as in the gecko *Hemidactylus bowringi* (Liu and Maneely 1969b), the long myotubes are reached by nerves that form ramified neuromuscular junctions (Hughes and New 1959). Thin fibers (0.5–1 μm) are believed to be sensory fibers, whereas thicker axons are believed to be motor fibers. A diffuse distribution of cholinesterases has

Fig. 2.6 (continued) located at the end of an elongating muscle fiber. *Bar* 2.5 μm. **d** Thymidine-labeled nucleus (*arrow*), at 12 days after injection of tritiated thymidine. The *arrowhead* points to a myofibril. *Bar* 1 μm. **e** Detail of a forming neuromuscular junction (*double arrowheads*) with deepening folds (*arrows*). Various dense core vesicles (*arrow*) are present in this end plate. *Bar* 200 μm. *mu* muscle cell/myotube, *nu* nucleus

been detected in myoblasts and also in myotubes, and the enzymes become restricted to the neuromuscular junction of mature regenerated muscles (Filogamo and Marchisio 1961; Sassu and Marchisio 1963; Shah and Chakko 1972). In most myofibers of the nonautonomous part of the tail, the neuromuscular junction (motor plaque) is localized in the medial/central part of the fiber. Conversely, in regenerating muscles the neuromuscular junction is present in the distal extremity of the fiber, close to the connective septa (Hughes and New 1959; Filogamo and Marchisio 1961; Sassu and Marchisio 1963; Gabella 1965). The first neuromuscular junctions are seen in long myotubes, localized by their extremities and more infrequently in the central part (Fig. 2.6d). This pattern of innervations seems to derive from the relatively late period in which the growing nerves reach the regenerated muscles in comparison with the more rapid innervation process that occurs during normal development. In fact, in regenerating muscles the growing nerves derived from the stump spinal cord or ganglia reach the new muscles at the stage of elongating mytotubes, containing various nuclei and numerous myofibrils. The neuromuscular junction is therefore established in the more immature part of the sarcoplasm, namely, at the extremity of the fiber. The late innervations during muscle regeneration explain the flaccidity and lack of contractility of the early regenerated tail, where numerous myotomes are already present

Ultrastructural studies have indicated that the motor end plate is immature at the extremity of regenerating fibers (Bottazzi-Bacchi and Sassu 1973; Alibardi, personal observations). Progressive stages of end-plate maturation have been described. From a small synaptic bouton contacting superficially the muscle fiber, an invaginated bouton is derived where the initial junctional folds are present (Fig. 2.6e). At later stages, the folds become deeper and the bottom surface is more extended in the more deeply located neuromuscular junction.

The process of myogenesis has been reproduced and analyzed in vitro (Simpson and Cox 1967; Cox 1969a, b; Simpson and Bayne 1979) using an initial growth medium for cell survival and proliferation, and later a fusion medium, favoring myotube formation and fiber differentiation. These studies on the lizard model of myogenesis have contributed to detailed knowledge of the process of myogenesis in vertebrates.

Fusiform myoblasts, derived from promuscle aggregates and cultivated for 8–9 days in the first growth medium, become rounded and the postmitotic cells enter the G1/G0 phase of the cell cycle, ready to merge into myotubes. In fact, whereas fusiform myoblasts take up tritiated thymidine, most of the round myoblasts do not take up this DNA precursor. The surface of round and prefusion cells shows numerous blebs or filopodia, and few of these cells have a smooth surface (Bayne and Simpson 1977). Instead, a smooth surface is generally typical of stretching myoblasts and forming myotubes. A specific cell antigen indicating muscle differentiation, indicated as Ag1422, is present in G0 phase and myosin-positive rounded myoblasts, but the antigen is absent in round myoblasts still capable of proliferation and that also appear to be myosin-negative (Marusich and Simpson 1983).

A detailed ultrastructural analysis of prefusion (round) myoblasts has shown the gradual formation of Z-bands, and has indicated that this is a useful system for the molecular analysis of myogenesis in general (Chlebowski et al. 1973; Bayne and Simpson 1977). This analysis has shown that the production of bundles of thin filaments of 7–8 nm (actin) precedes the appearance of the thick filaments of 12–14 nm (myosin). However, an equal number of thick (myosin) and thin (actin) bundles is rapidly produced in these cells as they differentiate, as confirmed by the immunoreactivity for myosin. Also acetylcholinesterase is present in some of the prefusion myoflasts (Simpson and Bayne 1979). This indicates that prefusion myoblasts are heterogeneous, in particular some are likely in G1 phase (acetylcholinesterase negative), whereas other myoblasts are in G0 phase (acetylcholinesterase positive). As these cells merge into myotubes, the immunoreactivity for myosin increases. The filaments assemble into myofibrils delimited by Z-bands forming sarcomeres that are arranged in linear rows, as observed in vivo (Fig. 2.6a, c, d). Some of the myosin-positive cells containing striated myofibrils can take up tritiated thymidine, suggesting that these nuclei may still divide, as observed in vivo.

2.2.4 Cartilage

The more apical 400–1,000 μm of the differentiating cartilaginous tube contains large extracellular spaces rich in acid mucopolysaccharides and relatively scarce fine fibrils of collagen synthesized from fusiform chondroblasts (Shah and Hiradhar 1975; Alibardi and Sala 1983). Initially in the blastema and in the precartilaginous aggregates, neutral or acidic but nonsulfated mucopolysaccharides are present, probably represented by hyaluronate, like in the amphibian blastema and cartilage (Toole and Gross 1971; Shah and Hiradhar 1975; Alibardi and Sala 1983; Alibardi, unpublished biochemical data).

From the precartilaginous aggregate in the regenerating cone until the elongating tail stage, numerous chondroblasts take up tritiated thymidine in both central and external regions of the cartilaginous tube (Figs. 1.6j, 2.7a). Therefore, cartilage growth occurs by both interstitial and appositional cell multiplication, although isogenic islands are rarely observed. The labeling index is higher in the apical regions and decreases in proximal regions of the cartilaginous tube (nearly one fifth of that in apical regions; Cox 1969a; Alibardi 1995b). In more proximal regions of the cartilaginous tube and near the old vertebra of the stump, the intercellular matrix becomes reduced around chondrocytes. In this region, few cells are seen to incorporate tritiated thymidine in both the inner region and the outer (external) region of the cartilaginous tube, suggesting that the growth of this region of the cartilaginous tube takes place slowly for both interstitial and appositional growth within the first month of regeneration (or at least until the new tail is completely scaled).

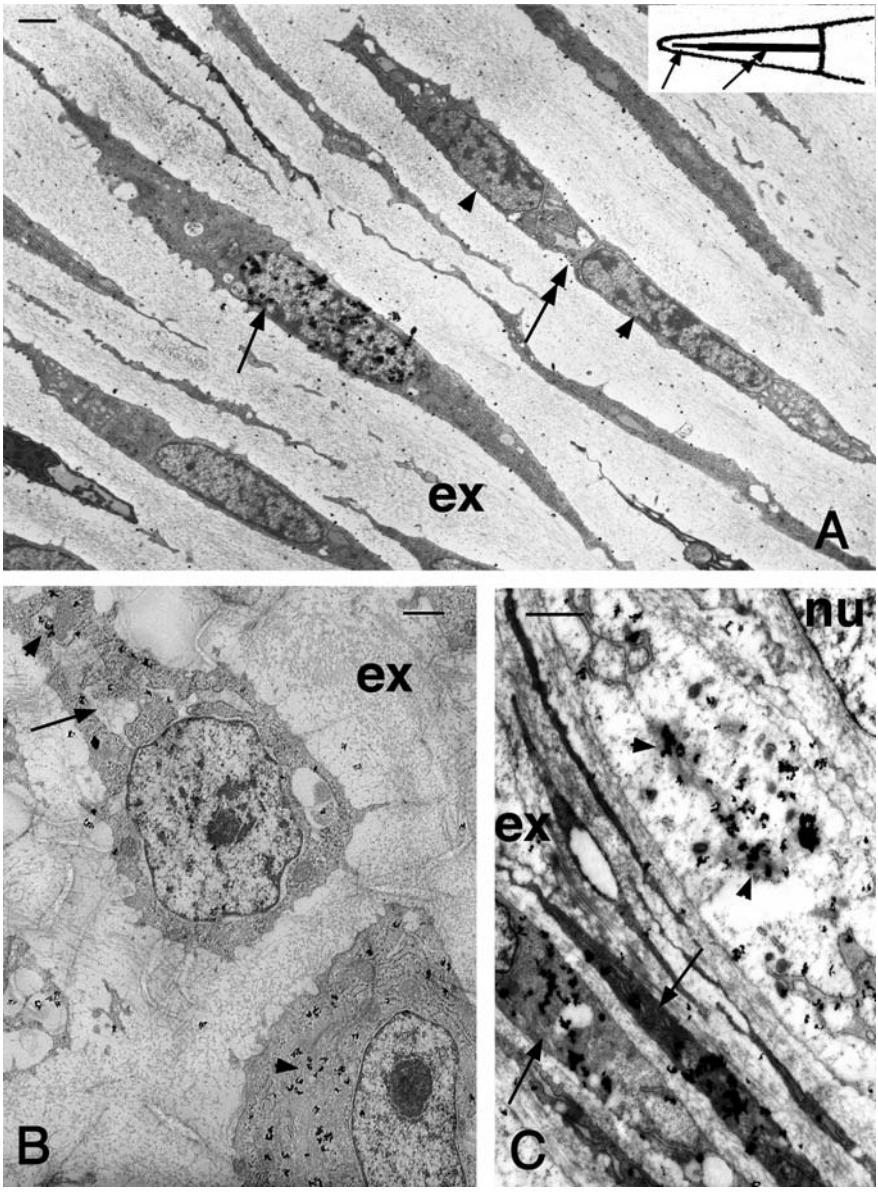

Fig. 2.7 Ultrastructural details of regenerating cartilage in *A. carolinensis* (**a**) and *L. delicata* (**b**, **c**). **a** Apical cartilage (*arrow* in the *inset*) showing a thin cell that has completed division (*arrowheads* on the nuclei; the *double arrow* indicates the separation cytoplasm in telophase). Another cell has a tritiated thymidine labeled nucleus (*arrow*). *Bar* 1 μm. **b** Two chondroblasts in the medial area of the cartilage (*double arrow* in the *inset* in **a**) with large ergastoplasmic cisternae (*arrow*) and incorporating tritiated proline (*arrowheads* on the

The early chondroblasts are metabolically very active cells as they take up tritiated proline in a higher amount in comparison with most epidermal cells, fibroblasts, adipose cells, and endothelial cells (Fig. 2.7b). Half an hour after injection of tritiated proline, the autoradiographic signals (dense curling silver trace grains) are mainly localized over the endoplasmic reticulum and the secretory cisternae (Fig. 2.7b). One hour after injection, the tracer is also abundant in the Golgi apparatus (Fig. 2.7c), but not outside chondroblasts. Three hours after injection, silver granules are also seen in the extracellular matrix and decrease inside chondrocytes (Alibardi 1995b). Therefore, the time of synthesis of collagen and acid mucopolysaccharides in lizard chondrocytes at the optimum temperature is similar to that for mammalian cells (Leblond 1991), although extrusion of labeled proteins appears to take somewhat longer in lizard cells.

When cartilaginous cells become more ovoidal or even rounded (Fig. 2.7b), about 1 mm from the apical tip of the regenerating cartilage in elongating tails, the cartilaginous matrix becomes richer in collagen fibrils and in sulfated mucopolysaccharides. This is indicated by the intensification of the periodic acid–Schiff stain reaction (collagen), by the appearance of metachromasia using toluidine blue, and by the reactivity to acidic alcian blue (indicating acid mucopolysaccharides with pI lower than 3) (Alibardi and Sala 1981, 1983). Other biochemical analyses (Alibardi, unpublished data) confirm the histochemical observations. The mature, mainly cellular cartilage only occasionally forms isogenic groups (two close chondrocytes), and chondroblasts remain isolated from one another.

The regenerated cartilaginous tube in most species so far analyzed is made of hyaline cartilage with a scarce matrix, which is responsible for most of the stiffness of the mature regenerated tail, especially after the cartilage has begun calcify. The formation of a hyaline cartilage with broad intercellular spaces and frequent isogenic groups has been noted in the lizard *Agama agama* (Alibardi and Meyer-Rochow 1989). Therefore, in most species of lizards the new tail is not very functional aside from having a balancing and lipid-storage function.

Differently from most lizards, in the gecko *Hemidactylus maculatus* elastic cartilage is formed instead of a stiff hyaline cartilage (Alibardi and Meyer-Rochow 1989). Chondrocytes become hypertrophic and contain very high amount of glycogen. Their Golgi apparatus produces dense vesicles that contain elastin, and the vesicles are extruded into the extracellular matrix that contains nonbanded collagen of undefined type. In more proximal and mature regions of the cartilaginous tube, the extracellular matrix contains many amorphous elastic bundles. The production of such an elastic cartilage, in conjunction with the

Fig. 2.7 (continued) silver grains) 1 h after injection. *Bar* 1 μm. **c** Detail of a maturing chondroblast contacting the fusiform cells of the external perichondrium (*arrows*). An intense labeling is also present in the Golgi apparatus (*arrowheads*) 1 h after injection of the radioactive precursor. *Bar* 0.5 μm. *ex* extracellular matrix, *nu* nucleus

formation of meninges rich in elastic fibrils (elastic meninges), allows the new tail of this gecko to curl up like the original tail. Therefore, the regenerating tail can be used for grasping and for climbing trees as this species is preferably arboreal.

Like in fractured bones of lizards (Pritchard and Ruzicka 1950), the replacement of cartilage tissue of the cartilaginous tube with bone occurs very slowly in lizards. Details of the process of calcification in mature regenerated tails are partially known (Calori 1858; Alibardi and Sala 1981; Alibardi and Meyer-Rochow 1989). In the more proximal regions of the cartilaginous tube, before calcification chondrocytes become hypertrophic and accumulate much glycogen. The process of calcification starts in the inner and outer cartilaginous rings in contact with the perichondrion (Fig. 1.7k, l). The replacement of degenerating chondrocytes initially occurs through the addition of new chondroblasts from the inner and the outer perichondrium, but later osteoblasts are produced in these ringlike regions where a true periosteum is formed as continuation of that of vertebrae (see the arrowheads in Fig. 1.7m). This process begins at 2–3 months after amputation in *Podarcis sicula* and at 6–8 months after amputation in *Sphenodon punctatus*. Calcium salts are initially deposited over the fine matrix grains, perhaps made of glycosaminoglycans, present among the collagen fibrils of the extracellular matrix in the outer and inner rings of the proximal cartilaginous tube (this occurs after 2 months from amputation in *P. sicula*). As a consequence, the cartilaginous matrix is destroyed and chondrocytes degenerate. Mineral deposits rapidly obscure the initial glycoprotein–collagenous network of the intercellular matrix. A true lamellar bone tissue slowly replaces the calcified cartilage and the inner and outer laminae.

2.2.5 Spinal Cord and Central Nerves

Aside from the apical ependymal ampulla where migrating cells seem to be loosely arranged (Fig. 1.4f, h), in more proximal regions ependymal cells form a close epithelium owing to the presence of numerous desmosomes (Simpson 1968; Egar et al. 1970). Ependymal cells are polarized with a relatively developed ergastoplasmic reticulum, Golgi apparatus, and numerous microvilli contacting the central canal during 2–4 weeks of regeneration. Numerous granules and vesicles containing glycoprotein material are secreted into the lumen (Turner and Tipton 1971; Alibardi and Sala 1986, 1989). Ependymal cells differentiate in more proximal regions of the spinal cord, at 2 mm from the tip and in regenerated tails over 4 weeks from the amputation. These cells initially terminate onto the basement membrane with a large base (Fig. 2.8a), but their basal part becomes thinner and branched as they mature. The latter cells present broad lateral spaces (tunnels in three-dimensional perspective) that are occupied by

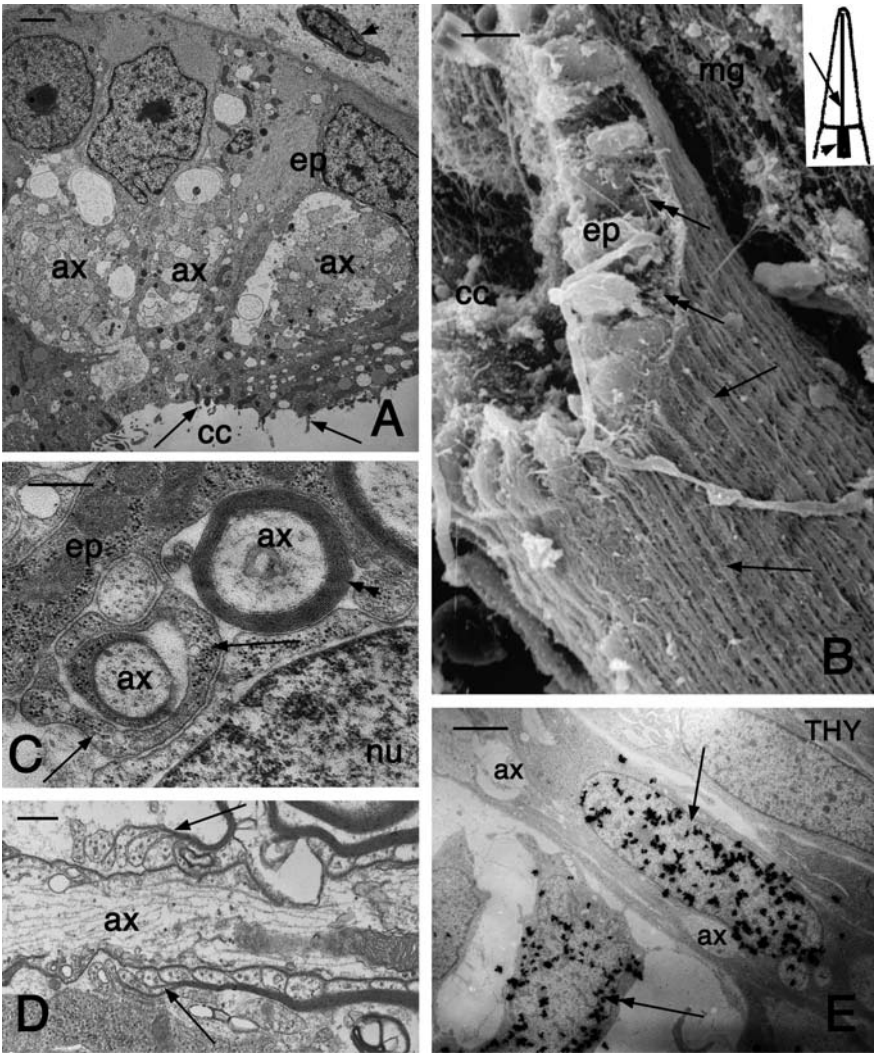

Fig. 2.8 Ultrastructural aspects of the regenerating spinal cord (**a**–**d**) and peripheral nerve (**f**). **a** Regenerated spinal cord of *P. sicula* in medial regions (see the indicative position in the *arrow* in the *inset* in **b**). The *arrow* indicates the luminal face and the *arrowhead* indicates the meninges. *Bar* 1 μm. **b** Scanning electron microscopic view of medial regenerated spinal cord in *A. carolinensis*. The *arrows* indicate collagen fibrils of the meninges. *Double arrows* indicate subpial spaces where the regenerating axons are located. *Bar* 10 μm. **c** Cross sections of two axons at the beginning of myelination (*arrowhead*) from elongation of ependymal tanycytes (*arrow*; 2 months of tail regeneration in *P. sicula*). B*ar* 250 nm. **d** Detail of a myelinating axon showing the terminal pedicels (*arrows*) of the oligodendrocyte in *Hemydactilus maculatus*. *Bar* 250 nm. **e** Two thymidine-labeled Schwann cells (*arrows*, 4 h after injection of the DNA precursor) surrounding a regenerating axon of *A. carolinensis*. *Bar* 1 μm. *ax* axons (located in among ependymal cells), *cc* central canal, *ep* ependymal cells, *nu* nucleus, *THY* tritiated thymidine labeling image

bundles of axons or axonal sections. Initially, ependymal cells act as a guide for the descending regenerating axons derived from the spinal cord stump (Simpson 1970, 1983). After 2 months of regeneration, ependymal cells tend to produce a narrow elongation containing bundles of intermediate filaments that terminate on the basement membrane, and are termed ependymal tanycytes (Simpson 1968; Alibardi 1990–1991). The basement membrane is in contact with regenerated meningeal cells and fibers, and the latter become numerous in regenerates over 2 months of age (Fig. 2.8b). From tanycytes, small elongations grow toward the axons and begin to enwrap the axons, so amyelinic or eventually truly myelinic axons are formed (Fig. 2.8c). In regenerates older than 2 months, numerous axons become myelinated from cells that have lost the epithelial organization and are recognizable as oligodendrocytes (Fig. 2.8d, e). Some of the myelinating cells are likely Schwann cells that have probably migrated into the regenerating spinal cord from actively dividing cells present around the growing nerves of the blastema (Fig. 2.8e) or from intracartilaginous nerves (Fig. 1.13a–d). Other glial cells are indicated as astrocytes, mainly owing to their pale cytoplasm and their elongation, that are rich in intermediate filaments, and by the lack of an axon and synaptic boutons.

The neuronal component of the new spinal cord is scarce and limited to specialized cerebrospinal fluid contacting neurons (CSFCNs). These small neurons are metabolically more active than ependymal cells, as indicated by their higher uptake of tritiated GABA and proline, which can probably circulate through the fenestrated blood vessels that surround the early regenerating spinal cord (Alibardi 1993b; Alibardi et al. 1993a, b). Neural nitric oxidase, the enzyme forming the neurotransmitter nitric oxide, is particularly abundant in these neurons innervating the growing blastema (Cristino et al. 2000a, b), but its role is not clear. Recent ultrastructural analysis has shown that CSFCNs are also regenerated in the reactive ependyma of the injured lumbar spinal cord before the ependyma becomes trapped with a glial scar. This observation indicates an intrinsic neurogenetic potential of the reactive ependyma of lizards at both tail and more rostral levels (Alibardi, unpublished observations).

CSFCNs have a pear-shaped body (12–18 μm), an electron-pale cytoplasm, sparse endoplasmic cisternae that sometimes form short Nissl bodies, and few axosomatic synaptic boutons (Fig. 2.9; Alibardi and Sala 1986, 1989; Alibardi and Meyer-Rochow 1988). These cells produce growth cones during their differentiation among ependymal cells. The presence of 90–120-nm-diameter large dense core vesicles, derived from the Golgi apparatus, indicates that these cells store and utilize catecholamines or, more likely, neuropeptides. CSFCNs possess a tuft of 2–6-μm-long stereocilia that contact the central canal and are more or less continuously regenerated. With use of tritiated thymidine autoradiography, it has been established that these cells derive from a few pale elements present among ependymal cells, and that they completely differentiate into CSFCNs in about 20 days (Alibardi et al. 1992; Alibardi 1993b). These neurons represent 5–10% of the entire cell population of the regenerating spinal cord at about

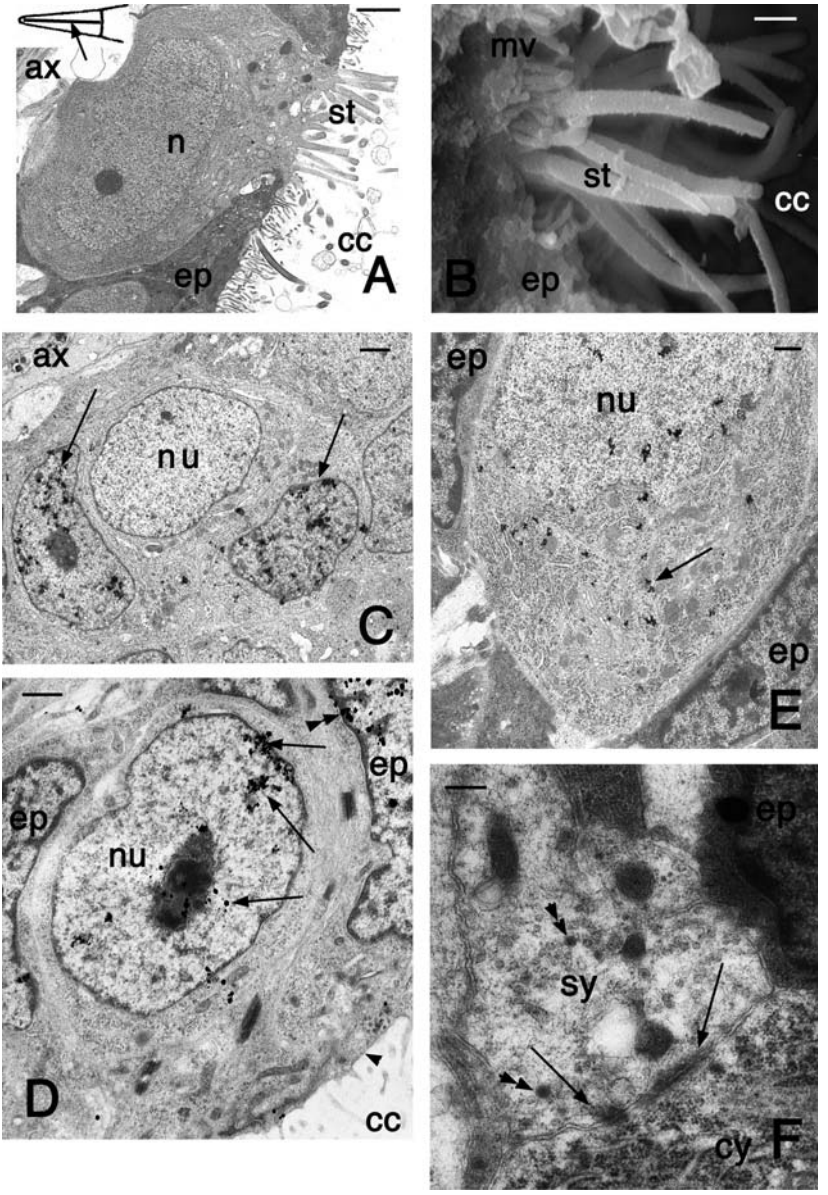

Fig. 2.9 Characteristics of regenerated cerebrospinal fluid contacting neurons (CSFCNs). **a** Pale CSFCN with tufts of stereocilia in the lumen of the central canal in *Leiolopisma nigriplantare maccanni*. The *inset* indicates the position of this cell in the regenerated spinal cord (*arrow*). *Bar* 2 μm. **b** Scanning electron microscope detail of the tuft of stereocilia of a CSFCN in *A carolinensis*. *Bar* 0.5 μm. **c** Differentiating CSFCNs between two tritiated thymidine labeled cells (*arrows*; 2 days after injection of the DNA precursor) in

1 month of tail regeneration (Fig. 2.10a): however, their number later decreases, probably owing to the isolation of the regenerated spinal cord inside the cartilaginous tube. During the tail elongation and maturation stages, neurons degenerate and are resorbed by ependymal phagocytes or by macrophages that have migrated into the spinal cord (Alibardi 1986). The number of CSFCNs increases after treatment with GABA, which seems to retard their degeneration (Alibardi et al. 1987). This suggests that under appropriate stimulation of the spinal cord, more CSFCNs may survive (see the later discussion).

The scarce numbers of axons present in the regenerating spinal cord mainly belong to descending axons and few axons form ascending pathways (Duffy et al. 1990, 1992). The ascending projections mainly derive from the few regenerated CSFCNs and appear to terminate on neurons present in the more proximal spinal cord in the stump (Duffy et al. 1992, 1993; Alibardi 1993a, b). Only a few long descending projections, largely originating from few a rhomboencephalic nuclei, reach down the regenerating spinal cord in the tail.

The descending or ascending axons are believed to form up to 2,000 axonal cross-areas, but this high number probably represents not individual axons but sprouting collaterals from descending axons coming from neurons of the stump (Duffy et al. 1990, 1992). Reactive motoneurons undergo a process of swelling during the first few weeks after amputation, with nuclear eccentricity and chromatolysis, all processes derived from the interruption of the axons from their target cells (Giuliani 1878; Marotta 1946; Baffoni 1950; Zannone 1953; Cristino et al. 2000a, b). These neurons later become hypertrophic and their nucleoli also increase in size. The hypertrophic motoneurons of the stump in particular increase their axosomatic synapse coverage since these cells receive more numerous terminals from descending axons of rostral sections of the spinal cord and even from the rhomboencephalon (Duffy et al. 1990).

The direct innervations of the regenerating tail, especially of the new muscles from the motoneurons within the last three segments of the spinal cord (roughly corresponding to the last three ganglia), have been shown using tract-tracing methods (Cristino et al. 2000a, b). No hypertrophic and labeled neurons were found in more rostral areas of the spinal cord (sacral, thoracic, and cervical).

Fig. 2.9 (continued) *L. delicata*. *Bar* 1 μm. **d** Lightly thymidine labeled nucleus (*arrows*) of a CSFCN (the *arrowhead* shows the contact with the central canal) 22 days after injection of the DNA precursor in *L. delicata*. A few silver grains (*double arrowhead*) are present over the chromatin of ependymal cells. *Bar* 1 μm. **e** Silver grains (*arrow*) from injected, tritiated GABA within CSFCNs. *Bar* 0.5 μm. **f** Detail of a synaptic bouton contacting a regenerated neuron. *Arrows* indicate the synaptic thickenings; The *double arrowhead* points to dense core vesicles. *Bar* 250 nm. *ax* axons, *cc* central canal of the ependymal tube, *cy* cytoplasm of postsynaptic neuron, *ep* ependymal cell, *nu* nucleus of CSFCN, *mv* microvilli, *st* stereocilia, *sy* synaptic bouton

Recent molecular analysis in geckos with a regenerating tail has shown that a potent inhibitor of axonal regeneration, identified as a myelin-associated glycoprotein precursor, is downregulated during the first 2 weeks of spinal cord regeneration (Liu et al. 2006). Therefore, a favorable environment is present in the lumbar and caudal spinal cord after transection. Another gene product, brain protein 44-like, is instead upregulated in the transected caudal spinal cord (Jiang et al. 2007). The activity of the latter gene seems to be linked to the stimulation of apoptosis, a process that is probably present during the first 2–3 weeks of spinal cord regeneration in lizards (Alibardi 1986; Alibardi and Sala 1986).

The connection between regenerated and normal spinal cord is quite limited, and even less with the brainstem. The presence of some neurons in rhomboencephalic nuclei, projecting to the regenerating spinal cord or to neurons in the proximal stump spinal cord of the tail, suggests that some mechanoreceptorial stimuli collected in the tail are transmitted to higher centers of the spinal cord and possibly to the brainstem. The resemblance of CSFCNs with inner hair receptors of the utriculus or sacculus has suggested that these neurons may be involved in monitoring the movement of the cerebrospinal fluid or of the Reissner fiber inside the ependymal canal (Alibardi and Meyer-Rochow 1988; Alibardi et al. 1993a). The latter role is not only supported by the cytological characteristics of these cells, but also by some experimental data (Alibardi et al. 1993a). Because these neurons are isolated within the cartilaginous canal, their survival chances decrease after 2 months of regeneration unless they are stimulated. This hypothesis has been tested by increasing the mechanosensory input to lizards during tail regeneration, leaving the animals in cages with 8–10 h/day of gentle but continuous rolling movement alternated with a circling movement for a period of 23 days after the formation of the regenerative blastema. These experimental conditions kept the lizards in continuous movement during the stimulatory period; in particular, the tail of these lizards tended to counterbalance the oscillatory and rotating movements of the body. This condition possibly increased the movement of the cerebrospinal fluid inside the ependymal canal. After 23 days in which lizards were regenerating their tail (6–10 mm long), the tail was analyzed histologically, counting the percentage of CSFCNs present in "stimulated" compared with normal lizards (Fig. 2.10b, c). These initial data indicated a small but significant increase of the percentage of CSFCNs in the experimental group in comparison with the normal group. The experiment suggests that a stimulating environment where more mechanical performances are required may enhance the survival of these cells, further pointing out that they may be receptors of fluid movement.

Other possible roles of CSFCNs within regenerated tails remain speculative, especially as possible trophic source of neurotrophic factors affecting tail regeneration. In fact, the dependence of tail regeneration on the regeneration of the spinal cord has suggested that some neurotrophic molecules released into the spinal fluid in the ependymal ampulla or into the surrounding cells of the blastema may have a possible role in stimulating tail regeneration and

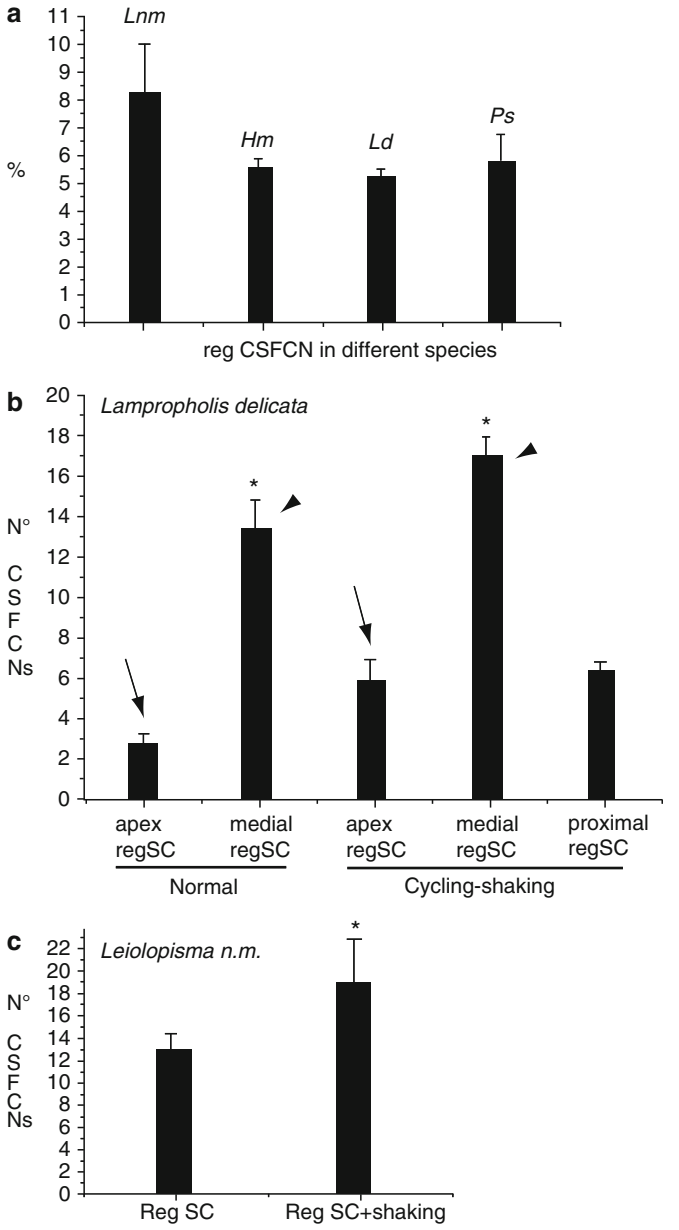

Fig. 2.10 The number of CSFCNs (percentage among ependymal cells, mean, and standard deviation) in different regions of the regenerating tail in normal conditions (**a**) along the entire regenerated spinal cord) and in experimental conditions (**b**, **c**). In **b** *arrows* and *arrowheads* indicate the comparison of the same region of the regenerated spinal cord for normal and experimental conditions. *Asterisks* indicate significant differences. In **c** the medial region of the regenerated spinal cord was counted for cells. *Lmn*, *L. nigriplantare maccanni*, *Ld*, *L. delicata*, *Ps*, *P. sicula*, *Hm*, *H. maculatus*

chondrogenesis (Simpson 1964; Alibardi et al 1988). Further work is, however, required on the latter problem.

2.2.6 Spinal Ganglia and Peripheral Nerves

The innervation of mesenchymal cells and myoblasts by nerves derived from spinal ganglia has been repeatedly observed (Hughes and New 1959; Filogamo and Marchisio 1961; Alibardi and Miolo 1990; Alibardi 1996b). The ultrastructural analysis has shown that many growing axons in the blastema store dense core vesicles of likely peptidergic content. These nerve terminals do not form synaptic specializations with blastema cells but release the content of these vesicles on the surface of blastema cells. Some blastema cells ensheating these terminals appear as Schwann cells mixed with other mesenchymal cells, and they give rise to nonmyelinated axons. Schwann cells actively take up tritiated thymidine and multiply around the growing nerves derived from the last three spinal ganglia in the stump.

In the normal tail, spinal ganglia produce two dorsal and two ventral branches that innervate the muscles and the skin belonging to three caudal segments of the tail, each corresponding to three scale verticals (Terni 1920; Fig. 1.1q). In the regenerating tail, the regenerated, segmental muscles are capable of contraction and are essentially innervated by motor and sensory nerves from the three closest ganglia of the stump, which extend their normal competence to many more targets.

The regeneration of some neurons in the two most proximal ganglia innervating the regenerating tail has been reported (Zannone 1953; Charvat and Kral 1969). However other studies performed using tritiated thymidine have shown that whereas satellite (glial) cells proliferate and increase in number, no new neurons are formed in the proximal ventral horns of the spinal cord or in the spinal ganglia during tail regeneration (Alibardi and Miolo 1990; Duffy et al. 1990, 1992; Alibardi 1995b). Also the tritiated thymidine labeled differentiated neurons observed in a few cases in both spinal cord and ganglia can, however, not indicate that these cells are actually proliferating. The significance of the labeling is related to the amplification of selected DNA fragments (genes) involved in axonal regeneration, and therefore a phenomenon of neuronal plasticity that allows hypertrophy and axonal sprouting (Borrione et al. 1991). In fact, ganglion neurons and those of the spinal cord stump only increase in dimension and cytoplasmic volume, and number of neurofilaments and other organelles including the synaptic input (Pannese 1963; Duffy et al. 1990, 1992; Geuna et al. 1992). Although hypertrophy affects most ganglion neurons, a subtype of ganglion neurons very rich in neurofilaments increased over other types in ganglia of regenerated tails (Geuna et al. 1992). The specific role of these neurons is, however, not known.

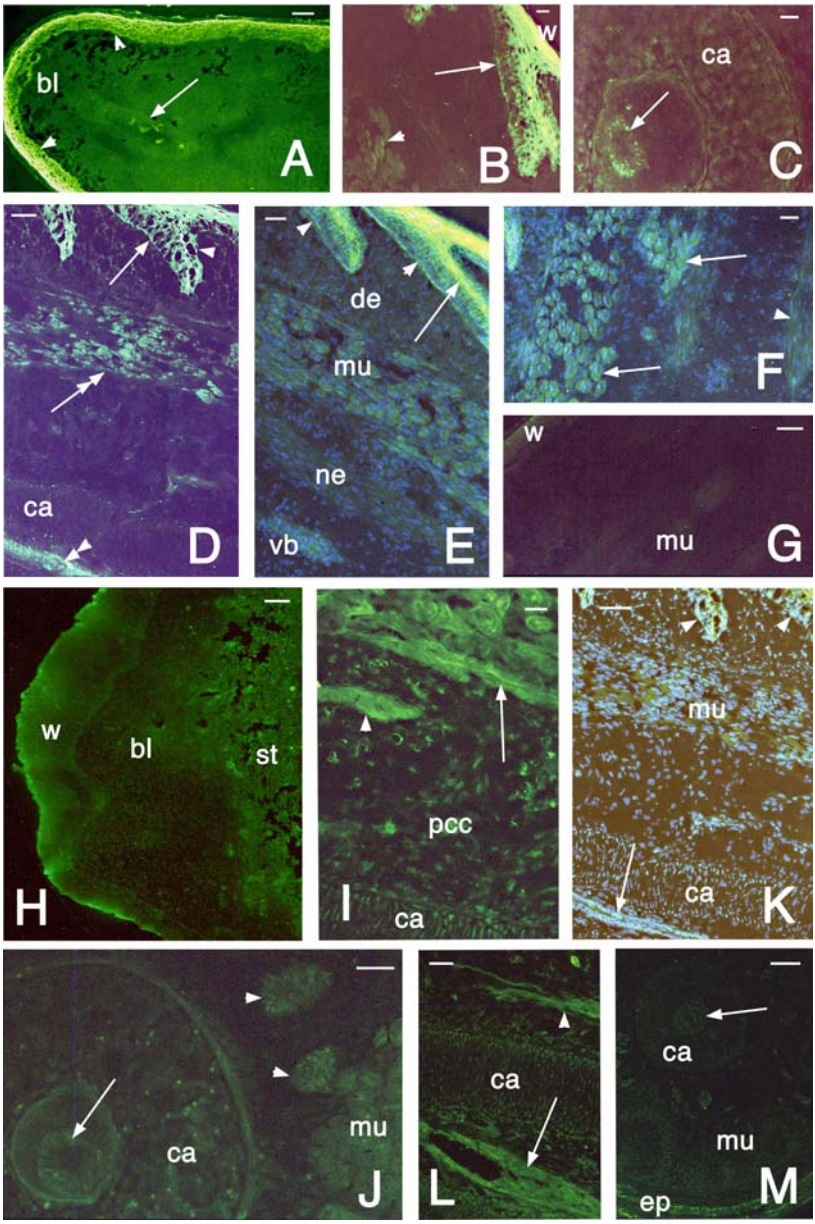

Fig. 2.11 Immunofluorescence localization of fibroblast growth factor 2 (FGF2) (basic, **a**–**g**) and fibroblast growth factor 1 (FGF1) (acidic, **h**–**m**) in the elongating tail of the lizard *L. delicata*. **a** Most immunofluorescence is seen in the wound epidermis (*arrowheads*) and ependymal tube. *Bar* 40 μm. **b** Detail of fluorescence-positive forming scale (*arrow*) and regenerating muscles (*arrowhead*). *Bar* 15 μm. **c** Cross sections showing a detail of

2.3 Growth Factors, Extracellular Matrix Proteins, and Keratins

2.3.1 Growth Factors

The localization, expression, activation, and general effects of growth factors on tissue regeneration in amphibians are known (Mesher 1996; Geraudie and Ferretti 1998; Gianpaoli et al. 2003). Recent studies have also extended this analysis to regenerating tissues in lizards (Alibardi and Loviku 2009). Few growth factors have been studied in the regenerating lizard tail and wounded limb.

Among other growth factors, fibroblast growth factor 1 (FGF1, acidic) and fibroblast growth factor 2 (FGF2, basic) are considered major stimulating molecules capable of replacing most of the activity of the neurotrophic factor as an inducer of organ regeneration in amphibians. The presence of FGF1 and FGF2 in the regenerating tail tissue of lizards has been shown by light and ultrastructural immunocytochemistry and immunoblotting (Alibardi and Loviku 2009, Alibardi, unpublished observations). Specific fibroblast growth factor reactive bands at 16–18 kDa have been identified only in the regenerating blastema and are not present or detectable in the normal tissues of both limb and tail.

The wound epidermis in the apical tail regions is immunofluorescent, whereas the blastema is poorly reactive for FGF2 (Fig. 2.11a). The apical ependymal ampulla and the more proximal regenerating ependymal tube are also immunolabeled (Fig. 2.11b, c). Also, the epidermal pegs of the forming scales, myoblasts aggregating to form segmental muscles, large regenerating nerves and their

Fig. 2.11 (Continued) an immunopositive ependymal tube (*arrow*). *Bar* 15 μm. **d** Longitudinal section of growing tail showing immunolabeled epidermal pegs (*arrow* on the proximal side, *arrowhead* on the distal side), muscles (*double arrow*), and ependyma (*double arrowhead*). *Bar* 16 μm. **e** Double-labeled fluorescence (nuclear labeling with 4′,6-diamidino-2-phenylindole (DAPI) and orange-yellow with fluorescein for FGF2). The *arrow* indicates the distal side and the *arrowheads* indicate the proximal side of epidermal pegs. *Bar* 15 μm. **f** Double labeling for FGF2 (*orange*) and nuclei (*blue*) for regenerating muscles in cross section (*arrows*). *Bar* 15 μm. **g** Nonreactive serum control. *Bar* 20 μm. **h** Blastema showing the higher labeling in the wound epidermis than in the blastema. *Bar* 15 μm. **i** Detail of immunofluorescent myotubes (*arrow*) and a blood vessel (*arrowhead*) within a regenerating tail. *Bar* 10 μm. **j** Cross section showing some labeling in the ependyma (*arrow*), and pericartilaginous nerves (*arrowheads*) and muscles. *Bar* 25 μm. **k** Double labeling for FGF1 (*orange*) and nuclei (*blue*). *Bar* 30 μm. **l** Detail showing the reactive ependyma (*arrow*) and peripheral nerve (*arrowhead*). *Bar* 15 μm. **m** Serum control (the *arrow* indicates the position of the immunonegative ependyma). *Bar* 25 μm. *bl* blastema, *ca* cartilaginous tube, *de* dermis, mu, muscles, *ne* nerve, *pcc* pericartilaginous connective tissue, *st* stump tissues, *vb* blood vessel, *w* wound epidermis

ganglia, and large blood vessels are immunolabeled (Fig. 2.11d, e). The immunofluorescence remains in the external sarcoplasm of growing muscle fibers and in the living epidermis of scales (the fluorescence of the corneous layers is nonspecific). The remaining tissues, such as cartilage, fat, and connective cells, do not show immunolabeling or are weakly labeled.

Within the medioproximal regions of the regenerating spinal cord, numerous immunolabeled nerves are seen, whereas ependymal cells are poorly or patchily labeled. Meninges surrounding the spinal cord appear weakly labeled or not labeled for FGF2. Neurons of the more proximal spinal cord in the stump, closer to the regenerating cord, show higher immunolabeling in comparison with neurons localized in the more distal spinal cord, far from the regenerating tissues (Alibardi and Loviku 2009). It is uncertain whether the few cell bodies showing immunoreactivity for FGF2 represent CSFCNs or macrophages within the ependyma. Control sections (preimmune rabbit serum or antigen-preabsorbed antibodies) confirm that the immunofluorescence is largely specific (Fig. 2.11g).

The antibody against FGF1 shows some reactivity to blastema cells and keratinocytes of the wound epidermis that are medium to strongly reactive (Fig. 2.11h). The apical ependymal ampulla and the more proximal ependymal tube inside the cartilaginous canal also show some immunofluorescence, whereas weak immunofluorescence is present in chondrocytes (Fig. 2.11i–l). FGF1 immunolabeling is also present in the nuclei of mesenchyme, of forming scales, muscles, and in the ependymal cells of the regenerating spinal cord, a different pattern from the immunolabeling for FGF2, where the nuclear labeling is much less evident. The FGF1 antibody also reacts with cells of the dermis beneath the forming scales, but poorly with the cartilaginous tube (except the perichondrium) and the surrounding connective-lipid tissue.

The large regenerating nerves derived from the proximal spinal ganglia are also immunoreactive for FGF1 (Fig. 2.11i, j). A more intense nuclear labeling is present in satellite and Schwann cells, but the labeling is less marked in ganglion neurons. In proximal regions of the regenerating tail at 4–5 weeks after amputation, immunoreactivity remains in the differentiating scales, muscles, and nerves, is scarce in the regenerating cartilage, and is absent in the dermis and pericartilaginous connective tissue. The immunofluorescence of cells in the proximal stump spinal cord is higher than in normal spinal cord. Some immunofluorescent axons in the regenerating spinal cord reach the apical ependymal ampulla (Fig. 2.11l). Control sections confirm that the labeling is largely specific (Fig. 2.11m).

Overall, the pattern of distribution of fibroblast growth factors in regenerating tissues of the lizard tail is similar to that of the regenerating limb and tail of the newt (Geraudie and Ferretti 1998; Gianpaoli et al. 2003). In the newt, FGF1 has been detected in both the wound epidermis, especially in the apical cup, as well as in blastema cells. It is believed that the apical cup produces FGF1, which stimulates the underlying cells of the blastema, or that blastema cells have an autocrine production of FGF1 that stimulates their own proliferation. Also, FGF2 is present

in the apical cup, especially its basal layer, and may stimulate blastema cell multiplication. Preliminary studies have indicated that whereas the wound epithelium of the tail and limb contains FGF2 at 2 weeks after amputation, the epithelium of the limb becomes immunonegative in later stages, in relation to the formation of scar connective tissue (Alibardi, unpublished observations).

TEM analysis (immunogold localization) has shown that FGF2 immunoreactivity is present in the extracellular matrix, especially near the apical wound epithelium contacting mesenchymal cells of the lizard blastema (Fig. 2.12a–c). It remains, however, unclear whether FGF2 moves from the epithelial cells to the mesenchyme or vice versa, and more dynamic studies are required to solve this question.

Fibroblast growth factor immunolocalization in the regenerating and differentiating muscle bundles suggests that such growth factors have autocrine stimulation for their own differentiation and growth. The presence of fibroblast growth factors in numerous blood vessels of the regenerating tail indicates the stimulation of angiogenesis by fibroblast growth factors in forming new blood vessels. The high expression of fibroblast growth factors in the spinal cord, ganglia, and nerves, aside from the stimulation of their own growth, may also be related to the possibility to release these growth factors in the growing blastema, where the factors may be acting as a neurotrophic agent. FGF1 is present in nuclei of reactive satellite cells within spinal ganglia innervating the new tail and this growth factor may stimulate their proliferation. In the regenerating spinal cord of the newt, FGF2 seems to stimulate the proliferation of neural stem cells in the regenerating ependyma (Zhang et al. 2000), and may also induce the proliferation and differentiation of ependymal cells into neurons. The latter effect has to be demonstrated for the lizard spinal cord. Therefore, these initial studies have also indicated that fibroblast growth factors may also be among the main candidates for a neurotrophic factor for tail regeneration in lizards, like in amphibians.

Also transforming growth factor beta-1 (TGF-β_1) and transforming growth factor beta-3 (TGF-β_3) in regenerating tail and limb have been immunolocalized in normal and regenerating limb and tail tissues (Alibardi, In press). TGF-β_1 appears localized in the connective tissue of the stump, but is appears diffusely present in mesenchymal cells of the blastema. A higher level of immunoreactivity is observed in the forming scar tissue of both tail and limb scars (Alibardi, unpublished observations). In this respect, it appears from the initial observations that also in lizards TGF-β_1 presents an overexpression pattern typical of scar tissues in mammals (Ferguson and O'Kane 2004). Preliminary data on TGF-β_3 of 20–22 kDa indicate it is upregulated in the regenerating blastema and in the dermis of the elongating tail, whereas this form is absent or is not detectable in normal tissues. Immunocytochemistry shows that among lesioned stump tissues, some connective cells are particularly rich in TGF-β_3 and they accumulate beneath the wound epidermis, but further analysis is currently in progress.

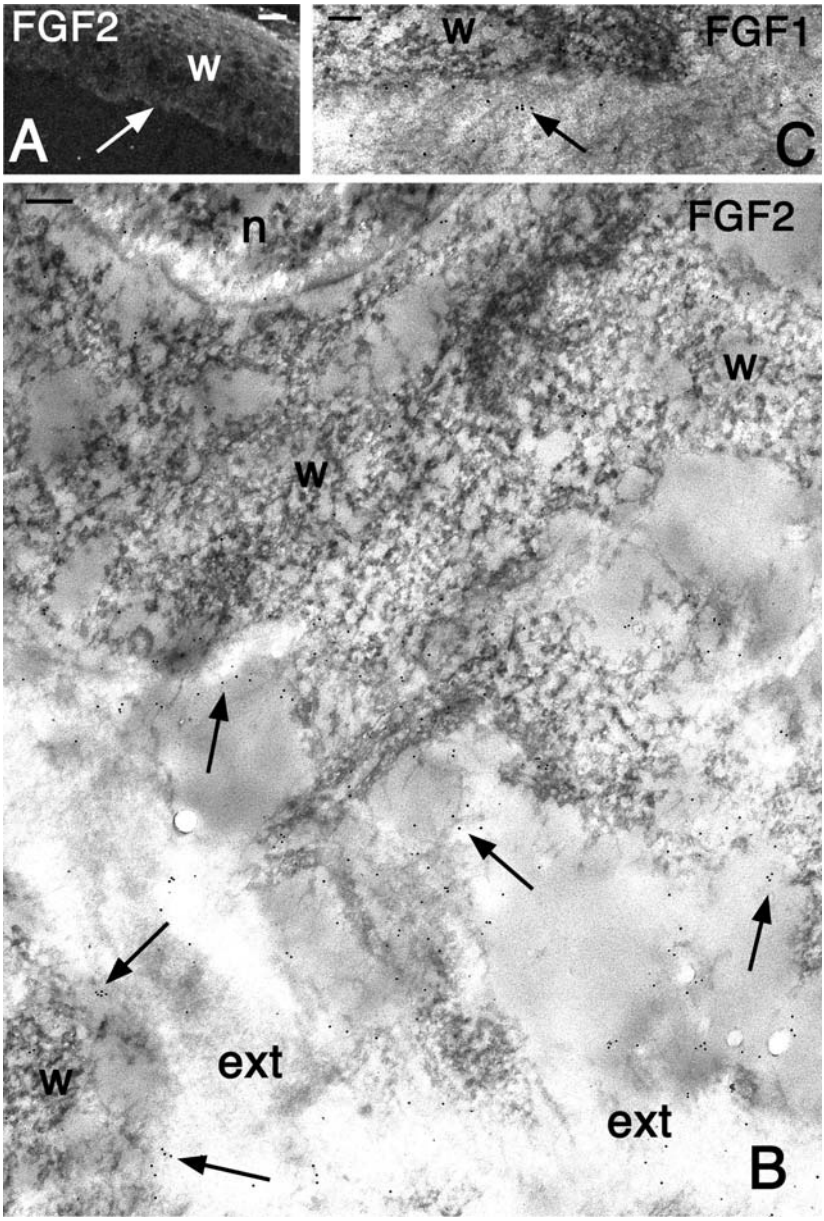

Fig. 2.12 Immunofluorescence (**a**) and immunogold localization (**b**, **c**) of FGF2 in the regenerating wound epithelium of the tail. **a** Immunolabeling along the (incomplete) basement membrane (*arrow*). *Bar* 10 μm. **b** Detail of immunogold labeling (*arrows*) along the basement membrane of wound epidermal cells. *Bar* 200 nm. **c** Detail of the labeling (*arrow*) along the basement membrane. *Bar* 100 nm. *ext* extracellular matrix, *FGF2/1* immunolabeling using FGF2/FGF1 antibody, *n* nucleus, *w* wound epithelium

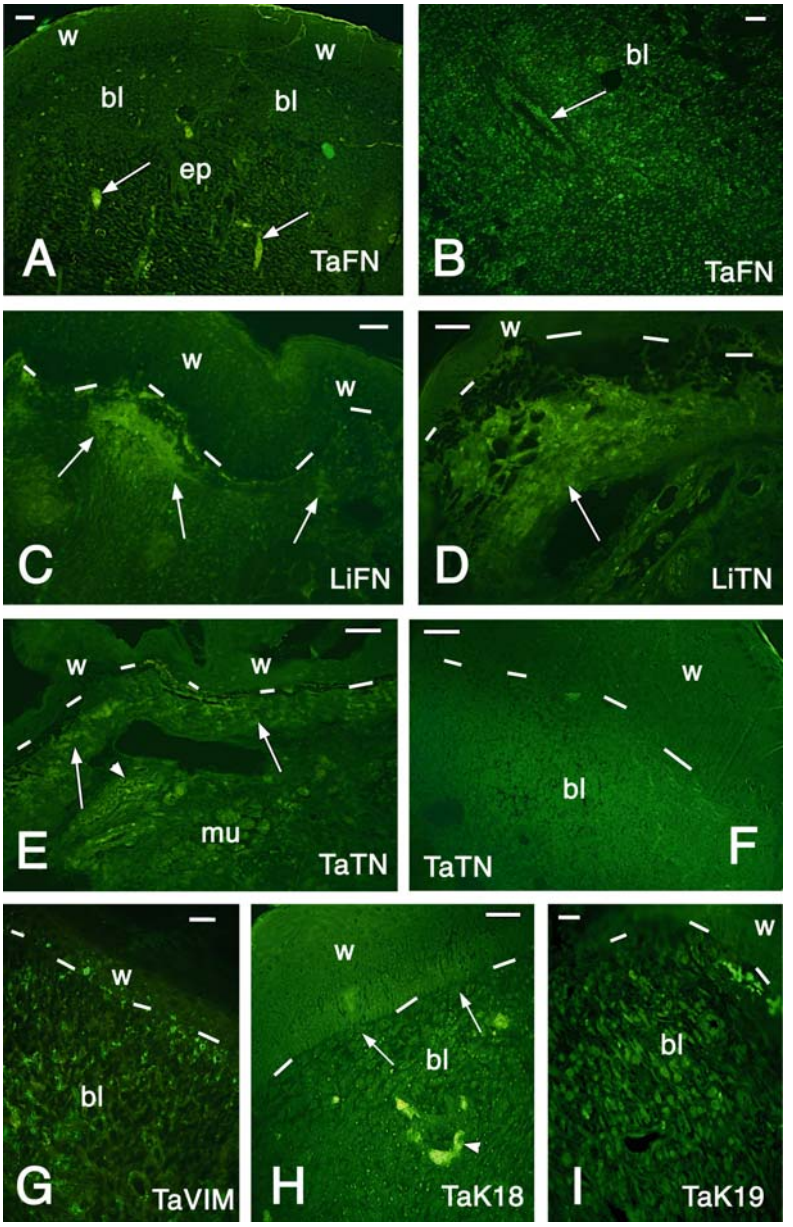

Fig. 2.13 Immunofluorescence images of regenerating tail (**a**, **b**, **e**–**i**) and limb (**c**, **d**) of *P. sicula*. **a** Tail at the cone stage showing a diffuse staining for fibronectin in the blastema but not in the wound epithelium. *Arrows* indicate nonspecific staining of blood vessels. *Bar* 10 μm. **b** Central region of the regenerating cone with fibronectin-immunostained mesenchymal cells and ependyma (*arrow*). *Bar* 15 μm. **c** Limb stump at 16 days after injury.

2.3.2 Extracellular Matrix Proteins

Fibronectin and ternascin are two of the main proteins of the extracellular matrix that have been implicated in the regeneration of amphibian limb and tail, and in the migration of the wound epithelium to cover the stump (see the summary in Geraudie and Ferretti 1998; Harty et al. 2003). Preliminary analysis has also been done in tissues of the lizard *P. sicula* (Alibardi, unpublished observations). Fibronectins of 220–240 kDa, and of lower molecular masses (perhaps degradative products), are present in the dermis of the wounded and regenerating tail and limbs, but not in the epidermis (Fig. 2.13a, b). Together, hyaluronate and fibronectin can stimulate the migration of mesenchymal cells toward the stump of the tail or limb. Also, ependymal cells of the apical ampulla appear to contain some fibronectin. This protein appears to be mainly localized in the connective tissue present beneath the wound epithelium that covers the limb stump at 12–20 days after amputation. The protein is not detectable in normal tissues or is only weakly detectable in the basement membrane of the epidermis. Like in the developing and regenerating limb of amphibians, fibronectin is largely expressed in the mesenchyme and later disappears where differentiating tissues, such as regenerating muscles and cartilage, are formed.

Lizard tenascin has a molecular mass of 220 kDa, although other immunoreactive bands at lower molecular masses are often present, but it is not known whether they represent degradation products. This protein is present in a low amount or is absent in the normal tail and limb connective tissues but becomes immunolocalized underneath the wounded dermis of both limb and tail stumps (Fig. 2.13c–e). The amount of this protein appears to increase in the limb stump beneath the migrating wound epithelium and in the forming basement membrane

Fig. 2.13 (continued) Fibronectin-immunopositive regions of the connective (*arrows*) are observed beneath the wound epithelium. *Bar* 15 μm. **d** Tenascin immunoreactivity in the connective tissue (*arrow*) located beneath the wound epithelium of a limb 13 days after amputation. *Bar* 20 μm. **e** Tenascin-immunoreactive forming blastema cells (*arrows*) 12 days after amputation. Immunofluorescence is also present in the dermis (*arrowhead*) located underneath the wound epithelium covering the tail stump. Also stump muscles appear immunostained. *Bar* 15 μm. **f** Tenascin-positive blastema cells in the tail and unlabeled thick wound epithelium. *Bar* 20 μm. **g** Vimentin-immunolabeled cells of the regenerating tail blastema. The wound epithelium is not labeled. *Bar* 15 μm. **h** Keratin 18 labeled blastema cells and in the wound epithelium (*arrows* on basal cells). *Bar* 20 μm. **i** Keratin 19 immunolabeled cells of the regenerative tail blastema and weakly in the wound epithelium. *Bar* 15 μm. *bl* blastema, *ep* ependymal tube, *LiFN* fibronectin labeling in the limb, *mu* muscles, *LiTN* tenascin labeling in the limb, *TaFN* fibronectin labeling in the tail, *TaK18/19* cytokeratin 18/cytokeratin 19 labeling in the tail, *TaTN* tenascin labeling in the tail, *TaVIM* vimentin labeling of the tail, *w* wound epithelium. *Dashes* underline the epidermis

underlying the nonapical regenerating epidermis. Tenascin immunoreactivity increases in the mesenchyme of the regenerating blastema but is absent in the wound epithelium (Fig. 2.13d). Tenascin has been implicated in the modulation of adhesion of fibroblasts to the epidermis, especially in the basement membrane underlying the wound epidermis.

Laminin of 210–220 kDa, well represented in the basement membrane of normal epidermis, disappears in the regenerative blastema, and is well detectable along the basement membrane of the elongating tail and in the dermis (probably linked to the blood vessel and muscle basement membrane). These preliminary data indicate that the increase of the amount of fibronectin and tenascin is a process that is needed for the migration of wound keratinocytes and the formation of a soft mesenchyme over the tail and limb stump.

2.3.3 Intermediate Filament Proteins

Vimentin and keratins are the main cytoskeletal intermediate filament proteins of the connective cells and epithelial cells, respectively. The presence of vimentin and keratins in the regenerative blastema of the tail has also been analyzed (Alibardi, unpublished data). Vimentin of 42 and 50 kDa is present in mesenchymal cells of the regenerating blastema, but the protein is absent in the wound epithelium (Fig. 2.13g). Vimentin is weakly detected or not visible in connective tissues of the normal tail.

The high expression of a 40–42-kDa keratin in the regenerating blastema or in the apical regions of the elongating tail (Alibardi et al 2000) and of wound keratins of 42–55 kDa (Alibardi and Toni 2005, 2006) has suggested that the mesenchyme of the blastema may contain keratins. This phenomenon was previously shown for the newt blastema (Corcoran and Ferretti 1997; Geraudie and Ferretti 1998). The presence of keratins 6, 16, and 17 in the regenerating tail has been associated with the contraction of migrating keratinocytes over the stump (Fig. 2.14).

Other keratins, however, are expressed more in the blastema than in the wound epithelium. In fact, both keratins 18 and 19 of 42 kDa are present in mesenchymal cells of the lizard blastema (Fig. 2.15h, i), a peculiar phenomenon previously reported for the regenerating blastema of the newt (Corcoran and Ferretti 1997). Keratin 19 is also a marker for stem cells, and the diffuse immunolabeling of blastema cells for this keratin suggests the presence of stem cells among those of the regenerative blastema. This preliminary observation is, however, being analyzed further. Therefore, it seems that also in the tail blastema of lizards, like in that of the newt, mesenchymal cells express typical simple keratins of epithelial tissues, indicating a reversion or dedifferentiation of the connective cells of the stump to embryonic cells (Corcoran and Ferretti 1997). This process in amphibians has been associated with the requirement of dedifferentiating cells to

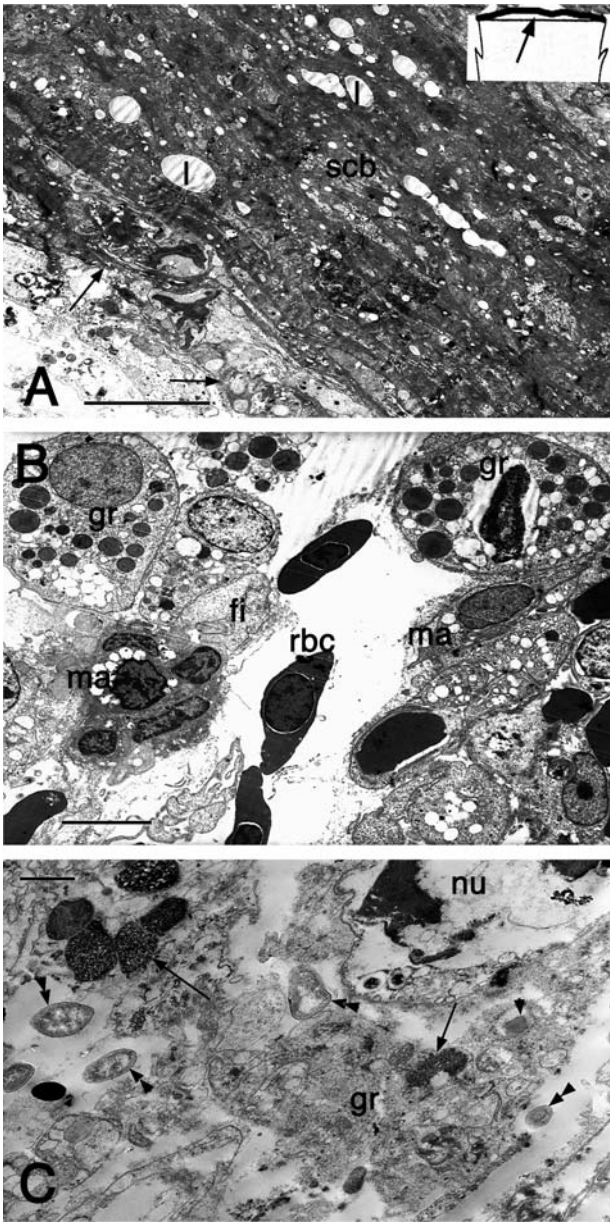

Fig. 2.14 Ultrastructural features of hindlimb stump at 4 days (**a**) and 7 days (**b**, **c**) after amputation in *P. sicula*. **a** Detail of the electron-dense and compact scab with degenerating leukocytes (*arrows*) localized underneath (position indicated by the *arrow* in the *inset*). *Bar* 1 μm. **b** Detail of granulation tissue rich in granulocytes and macrophages among few fibroblasts. *Bar* 3 μm. **c** Detail of spongy-like azurophil granules of granulocytes (*arrows*) that have engulfed some bacteria (*double arrowheads*). *Bar* 250 nm. *l* lipid vesicle, *fi* fibrocyte, *gr* granulocyte, *ma* macrophage, *nu* degenerating nucleus, *rbc* red blood cell, *scb* scab

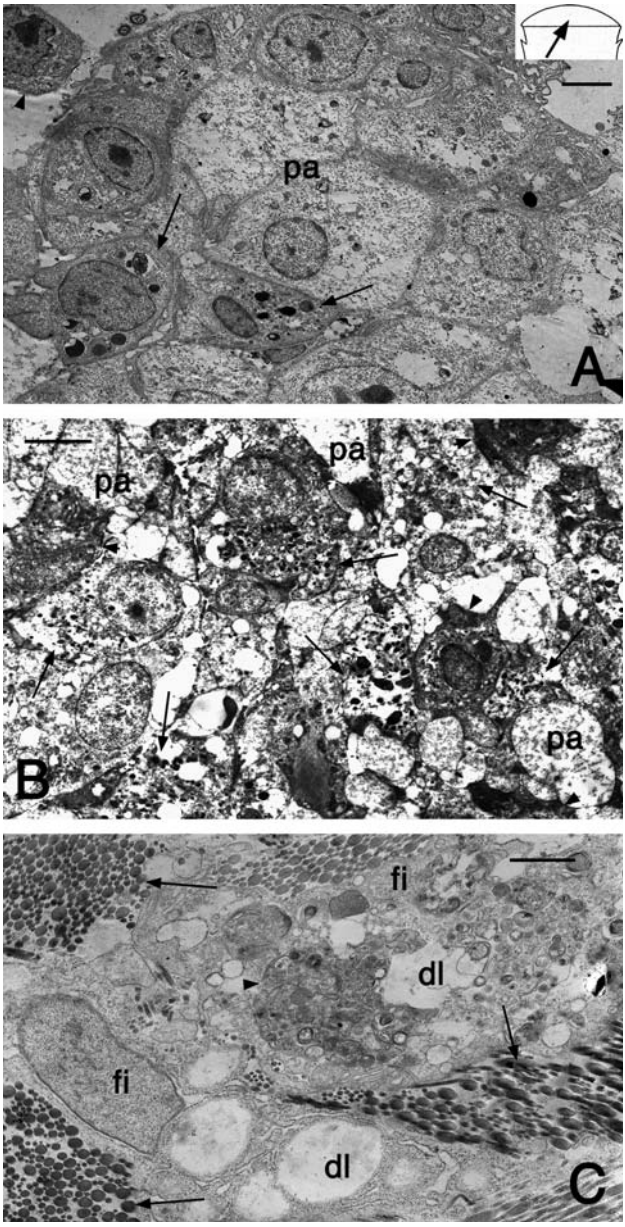

Fig. 2.15 Ultrastructural features of hindlimb stump at 13 days (**a**), 16 days (**b**), and 20 days (**d**) after amputation in *P. sicula*. **a** Epithelioid group of cells located in stump connective tissue, as indicated by the *arrow* in the *inset*. Among pale cells three phagocytes (*arrows*) are seen. A macrophage (*arrowhead*) is contacting this group of cells. *Bar* 1 μm. **b** Area of degenerating cells (*arrowheads* on dark cells) localized beneath the wound epidermis. *Arrows* indicate pale phagocytes rich in granular lysosomes. *Bar* 2.5 μm. **c** Detail of fibrocytes and a macrophage (*arrowhead*) surrounded by large collagen bundles (*arrows*). *Bar* 2 μm. *dl* degenerating lipid vesicles, *fi* fibrocyte, *pa* pale cell

produce a blastematic mass that recapitulates the stages of normal development of the limb (Geraudie and Ferretti 1998). However, this preliminary observation in lizards may also indicate that some blastema cells are derived from an epithelial–dermal transformation, since these epithelial keratins are conserved in mesenchymal-shaped cells. The latter, preliminary observations are presently being analyzed further.